

**PHENIX Beam Use Proposal
for RHIC Run-9 and Beyond
April 18, 2008**

The PHENIX Collaboration

Abstract

We present a multi-year program to quantify the nature of nuclear matter at the highest temperatures and densities, to search for the onset of the perfect liquid, locate the QCD critical point, and to increase our understanding of the elusive spin of the proton. Our plan takes full advantage of PHENIX detector upgrades and accelerator luminosity developments. Information on the current status of the experiment, on the data sets recorded to date, and on the program of proposed upgrades is also provided.

1 Executive Summary

The PHENIX Collaboration proposes a two-pronged scientific program to continue to exploit the discovery potential of RHIC. Precision measurements are key to quantifying the properties of the perfect liquid at RHIC and for determination of ΔG with increased sensitivity. In parallel, new scientific questions raised by RHIC data are addressed with enhanced experimental capabilities and higher luminosities.

Building upon the successes of Runs 1-8, the requested running conditions for heavy ion collisions will extend measurements of hard processes from the qualitative to the quantitative. New detector subsystems will allow heavy quark spectroscopy and extend the kinematic range of pion, direct photon, and photon-jet correlation probes. A new theme from Run-10 onward is running at lower energies to search for the onset of opacity and flow characteristic of the perfect liquid, and to look for experimental signals of the critical point of the QCD phase transition.

The PHENIX Collaboration considers it imperative to collect new spin data in FY2009 in order to maintain the vitality of the RHIC spin program. This is particularly true in light of new experimental opportunities at other facilities, and the dawn of an era where RHIC data provide substantial constraints to global analyses of the spin structure of the proton. Timely development of 500 GeV operations is requested to measure flavor dependent anti-quark polarization as well as reach lower x for ΔG .

In the out years, planned detector upgrades become available. Substantial data sets with full energy Au+Au, together with p+p and d+Au data for comparison, are needed

to utilize the new capabilities and observables provided by these upgrades. Full exploitation of these new detector systems will be further enhanced by the increased luminosities expected from stochastic cooling for Au+Au and improved polarization, beta-star, luminosity and spin-flip hardware in p+p.

We present in this document a five year run plan. The highest priority for the PHENIX Collaboration in Run-9 is to collect data with polarized protons, preferably at 200 GeV. Our goal is to record 25 inverse picobarns of data to substantially improve sensitivity to ΔG in neutral and charged pion A_{LL} measurements. We estimate that this will require 10 weeks of physics running. Should a Continuing Resolution prohibit 10 weeks of physics plus the necessary 5 weeks cooldown/setup/rampup before the end of June, PHENIX requests instead a first run of 500 GeV polarized proton collisions. In this event 3-4 weeks of physics running should be sufficient for first measurements of production cross-sections, background rates, and an initial W asymmetry measurement. The p+p collision energy that is not run in Run-9 would then be a priority for Run-10.

Our second priority for Run-9 is to record approximately 1.4 inverse nanobarns of Au+Au collisions. This will complete the large pre-LHC Au+Au data set and, most importantly, provide low mass dilepton spectra of sufficient precision to search for modification in ρ , ω and ϕ meson spectral functions. 8-10 weeks of Au+Au physics running should provide 1.2 to 1.4 nb^{-1} recorded integrated luminosity, and allow PHENIX to proceed with installation of the silicon vertex detector prior to Run-10. As the Hadron Blind Detector cannot coexist in PHENIX with the silicon vertex detector currently under construction, it is imperative to collect the required data now, so that PHENIX will be ready to utilize the vertex detector as soon as it is complete. We anticipate the first engineering run for the VTX pixel layers in Run-10.

For Run-10, the highest priority of the PHENIX Collaboration is to complete the second p+p goal. Should 200 GeV p+p be run in Run-9, then we require 500 GeV p+p collisions early in Run-10. This is necessary to provide data to meet the March 2011 milestone of our RIKEN collaborators for first observation of W's in the PHENIX muon arms. Our second priority in Run-10 is to begin the search for onset of the perfect liquid. We will accomplish this by measurement of the opacity of the produced medium to both light and heavy quarks, as well as the elliptic flow for identified hadrons in Au+Au collisions at energies between 62.4 and 22 GeV per nucleon pair.

We anticipate completion and installation of the VTX detector before Run-11. Consequently, it will be imperative to run full energy Au+Au collisions in Run-11 for the physics program of that vital upgrade.

2 Introduction

The goals of the PHENIX Collaboration for RHIC running have been clearly delineated in our previous Beam Use Proposals and presentations to the Program Advisory Committee[1, 2, 3, 4, 5, 6, 7, 8, 9, 10]. The consistent theme is the need for the highest possible integrated luminosities (and polarizations in the case of p+p running) to explore fully the range of fundamental phenomena in nucleus+nucleus, “proton”+nucleus and proton+proton collisions. The requested program has been designed to provide incisive measurements necessary to understand the spin structure of the proton and the nature of nuclear matter at the extremes of temperature and density, while performing the necessary baseline measurements for both the spin and the heavy ion programs.

Every effort has been made to keep PHENIX’s triggering, data acquisition and archiving abilities well matched to the delivered luminosity. We are currently undertaking R&D to develop upgrades that will keep the PHENIX data acquisition and triggering capabilities matched to the increased luminosity expected in 2012. We have been extremely successful in providing timely analysis of our data-sets using not only the RHIC Computing Facility (RCF), but also the very significant computing resources from PHENIX institutions in the United States (LLNL, New Mexico, ORNL, Vanderbilt), Japan (“CC-J”) and France (“CC-F”).

PHENIX had two successful data taking periods in Run-7 and Run-8. We collected Au+Au data exceeding previously available statistics by a factor of 4. As our combined goal for Run-7 + Run-9 is to increase the sample size by an order of magnitude to investigate rare probes prior to LHC start-up, we anticipate completing the required data set in Run-9. Run-7 served as an engineering run for the Hadron Blind Detector. Problems in the high voltage distribution, discussed further below, limited the acceptance covered by functioning detector sectors during Run-7. The problems have been solved and we will do the high quality low mass dilepton measurement in the next Au+Au run. This goal is well-matched to the integrated luminosity requirement for completion of the order of magnitude larger Au+Au data set.

The d+Au data collected in Run-8 is a factor of 30 larger than that available from the last d+Au run in 2003. This provides definitive comparison data for our Au+Au measurements in Run-4 and Run-7. Polarized proton collisions in Run-8 allowed PHENIX to approximately double the modest sample of transversely polarized proton-proton collisions collected in Run-6. We also added to the p+p reference data for the Muon Piston Calorimeter which was collected in Run-6.

PHENIX has made significant progress in both the heavy ion and the spin programs despite curtailed running time in each of Runs 6 through 8. Nevertheless, the missing weeks do add up. This is particularly notable in the spin program, which has had no substantial running since Run-6. The lack of polarized p+p running has also had a

deleterious effect upon polarization and luminosity development goals, slowing progress toward the levels assumed in the RHIC Spin Research plan[11].

We present in this document a five year run plan beginning with Run-9 that will allow us to:

- Substantially improve sensitivity to ΔG via high statistics neutral and charged pion A_{LL} measurements.
- Complete an order of magnitude larger Au+Au data set prior to LHC turn-on, allowing utilization of hard probes to quantify properties of the perfect liquid.
- Measure low mass dilepton spectra with high precision to determine the mass, p_T , and centrality dependence of the low mass excess observed in Run-4.
- Search for the onset of the perfect liquid.
- Measure the parity violating production of W bosons to investigate anti-quark polarization.
- Utilize new detector sub-systems and enhanced RHIC luminosity to separate charm and bottom quarks and quantify the mass-dependence of the stopping power of the perfect liquid.
- Study U+U collisions to substantially increase the energy density over that achievable in Au+Au.
- Search for the location of the QCD critical point.

3 Status of the PHENIX Experiment

The PHENIX detector has evolved from a partial implementation of only the central arms in Run-1, a completed installation of the baseline + AEE (Additional Experimental Equipment) systems for Run-3, to a significantly enhanced detector from Run-4 onward. Crucial upgrades were added for Run-7, and additional strategic upgrades are either under construction, or nearing construction start.

Table 1 summarizes the data collected in Runs 1-8. For each data-set the “*proton+proton equivalent*” “*recorded*” integrated luminosity is given by the corresponding column of the table. For an $A+B$ collision the *proton+proton equivalent* integrated luminosity is given by

$$\int \mathcal{L} dt|_{p+pequivalent} \equiv A \cdot B \int \mathcal{L} dt|_{A+B} \quad ,$$

Run	Year	Species	$\sqrt{s_{NN}}$ (GeV)	$f L dt$	N_{Tot}	p+p Equivalent	Data Size
01	2000	Au+Au	130	1 μb^{-1}	10M	0.04 pb^{-1}	3 TB
02	2001/2002	Au+Au	200	24 μb^{-1}	170M	1.0 pb^{-1}	10 TB
		p+p	200	0.15 pb^{-1}	3.7G	0.15 pb^{-1}	20 TB
03	2002/2003	d+Au	200	2.74 nb^{-1}	5.5G	1.1 pb^{-1}	46 TB
		p+p	200	0.35 pb^{-1}	6.6G	0.35 pb^{-1}	35 TB
04	2004/2004	Au+Au	200	241 μb^{-1}	1.5G	10.0 pb^{-1}	270 TB
		Au+Au	62.4	9 μb^{-1}	58M	0.36 pb^{-1}	10 TB
05	2004/2005	Cu+Cu	200	3 nb^{-1}	8.6G	11.9 pb^{-1}	173 TB
		Cu+Cu	62.4	0.19 nb^{-1}	0.4G	0.8 pb^{-1}	48 TB
		Cu+Cu	22.5	2.7 μb^{-1}	9M	0.01 pb^{-1}	1 TB
		p+p	200	3.8 pb^{-1}	85G	3.8 pb^{-1}	262 TB
06	2006	p+p	200	10.7 pb^{-1}	230G	10.7 pb^{-1}	310 TB
		p+p	62.4	0.1 pb^{-1}	28G	0.1 pb^{-1}	25 TB
07	2007	Au+Au	200	0.813 nb^{-1}	5.1G	33.7 pb^{-1}	650 TB
08	2008	d+Au	200	80 nb^{-1}	160G	32.1 pb^{-1}	437 TB
		p+p	200	5.2 pb^{-1}	115G	5.2 pb^{-1}	118 TB

Table 1: Summary of the PHENIX data sets acquired in RHIC Runs 1 through 8. All integrated luminosities listed are *recorded* values.

which corresponds to the integrated parton+parton luminosity, without taking into account any nuclear enhancement or suppression effects. The *recorded* integrated luminosity is the number of collisions actually examined by PHENIX, as distinguished from the larger value delivered by the RHIC accelerator. In the case of minimum bias data sets, “recorded” is strictly accurate, while for triggered data “sampled” more accurately describes the process. We use “recorded” as shorthand for either case to refer to the number of events examined by PHENIX for a given physics observable

In the period of late 2007 and early 2008 PHENIX submitted seven new papers for publication. arXiv:0801.4555[12] showed the results of a first energy scan to search for the onset of jet quenching in the hot, dense medium created in heavy ion collisions. The search was done by measuring the nuclear modification factor R_{AA} , which is the ratio of yield in ion collisions compared to that expected from the commensurate number of p+p collisions, of π^0 's at several energies. Figure 1 shows that, in Cu+Cu collisions, strong jet quenching (i.e. suppression of high momentum particle production) is observed in 200 and

62.4 GeV per nucleon pair collisions, but there is no suppression at 22.4 GeV. The presence of nuclei actually enhances particle production. This enhancement, the "Cronin effect" long known in collisions at several tens of GeV, may mask the presence of some energy loss of quarks and gluons in 22.4 GeV heavy ion collisions. However, the observed change from strong suppression to no suppression clearly shows that the remarkable opacity of the hot, dense medium of quarks and gluons discovered at RHIC has an onset somewhere between 22.4 and 62.4 GeV per nucleon pair collision energy. Future energy scans at RHIC should be used to pinpoint just where the onset is, and determine the properties of the medium at that energy.

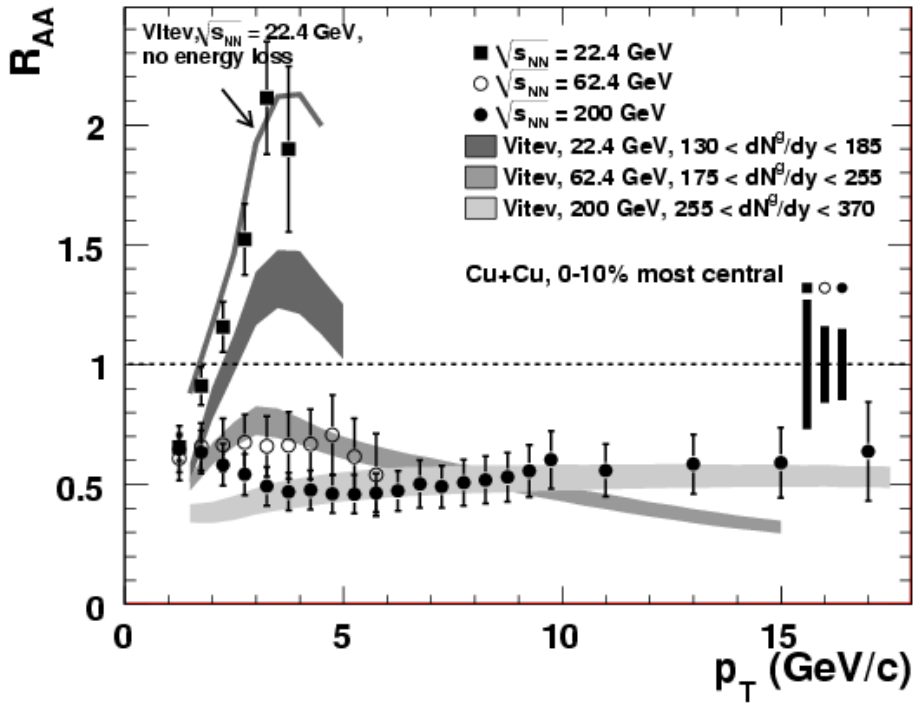


Figure 1: Measured π^0 R_{AA} as a function of p_T for the 0 – 10% most central Cu+Cu collisions at $\sqrt{s_{NN}} = 22.4, 62.4, 200$ GeV in comparison to a jet quenching calculation [13]. The error bars represent the quadratic sum of the statistical uncertainties and the point-to-point uncorrelated and correlated systematic uncertainties. The boxes around unity indicate uncertainties related to $\langle N_{\text{coll}} \rangle$ and absolute normalization. The bands for the theory calculation correspond to the assumed range of the initial gluon density dN^g/dy . The thin solid line is a calculation without parton energy loss for central Cu+Cu at $\sqrt{s_{NN}} = 22.4$ GeV.

Other new PHENIX publications report on the fate of J/ψ in Cu+Cu collisions[14] (arXiv:0801.0220), show the spectra and suppression of neutral pions to 20 GeV/c transverse momentum in Au+Au[15], illustrate how to quantify energy loss parameters in different models by careful control of the different kinds of experimental uncertainties[16],

map out the correlations of jet fragments as a function of transverse momentum to study the medium response to deposited energy[17], provide three dimensional images of the final state of the medium in Au+Au as it breaks up[18], and present the first measurement of di-electrons in p+p collisions at RHIC, using these to extract the heavy quark production cross sections[19].

3.1 Achievements in Run-7 and Run-8

PHENIX had two very successful data taking periods in Run-7 and Run-8, collecting a Au+Au data set in Run-7 that exceeded our previous statistics by nearly a factor of 4.

Reconstruction of the Run-7 minimum bias data set has been completed; preliminary results from approximately 75% of the data set were shown at the recent Quark Matter 2008 conference in Jaipur in February. Reconstruction of the muon arm data from Run-7 is about 40% complete, and is expected to finish in approximately 2 months. Remarkably, PHENIX continues to be able to fully reconstruct the entire data set within a year of the end of each run, even in the current era of data sets over half a petabyte per year.

The d+Au data collected in Run-8 is a factor of 30 larger than that available from the last d+Au run in 2003. Over 80 pb^{-1} of integrated luminosity was sampled, representing 160 billion minimum-bias events. This data set will provide a much needed precision reference for cold nuclear matter effects upon probes of the hot, dense matter produced at RHIC. In particular, the conclusions from J/ψ and open charm production will become much clearer using the Run-8 data to remove one of the dominant uncertainties on the rapidity and \sqrt{s} dependence of $J\psi$ suppression. The new d+Au data will also allow PHENIX to better quantify the Cronin effect in the central arm. The extent to which the baryon enhancement in d+Au exceeds the meson enhancement, along with possible saturation of the enhancement with the number of nucleon-nucleon collisions, will allow PHENIX to solve the several decade long mystery of whether the Cronin effect is due to initial state multiple scattering in the target nucleus. Utilizing the TOF-West and Aerogel counters, which were not available in Run-3, will provide particle identification to much higher p_T than previously possible. PHENIX had two Muon Piston Calorimeters in place during Run-8, allowing a search for evidence of saturation of gluons in nuclei at small momentum fraction. Because of its short duration, low polarization and luminosity, and lack of radial polarization development, the p+p running in Run-8 allowed PHENIX only to double the modest-sized transverse polarized p+p statistics from Run-6. Nevertheless, we will combine the two data samples and study the interference fragmentation function and Sivers effect in the transverse polarized proton-proton collisions. Reconstruction of the Run-8 data has just begun.

3.2 Run-7 Additions to PHENIX

PHENIX installed significant upgrades for Run-7: the Reaction Plane Detector (RXNP), Time of Flight-West (TOF-W), Muon Piston Calorimeter-North (MPC-N) and the Hadron Blind Detector (HBD). These are shown installed in PHENIX in figure 2. MPC North was the second MPC, so this detector system was complete from Run-7 onwards. Run-7 served as an engineering/commissioning run for the HBD and a physics run the other three new detector subsystems. The successful operation of these three new subsystems has resulted in an expansion of the physics capabilities of PHENIX in a number of important areas in both heavy ion and spin physics.

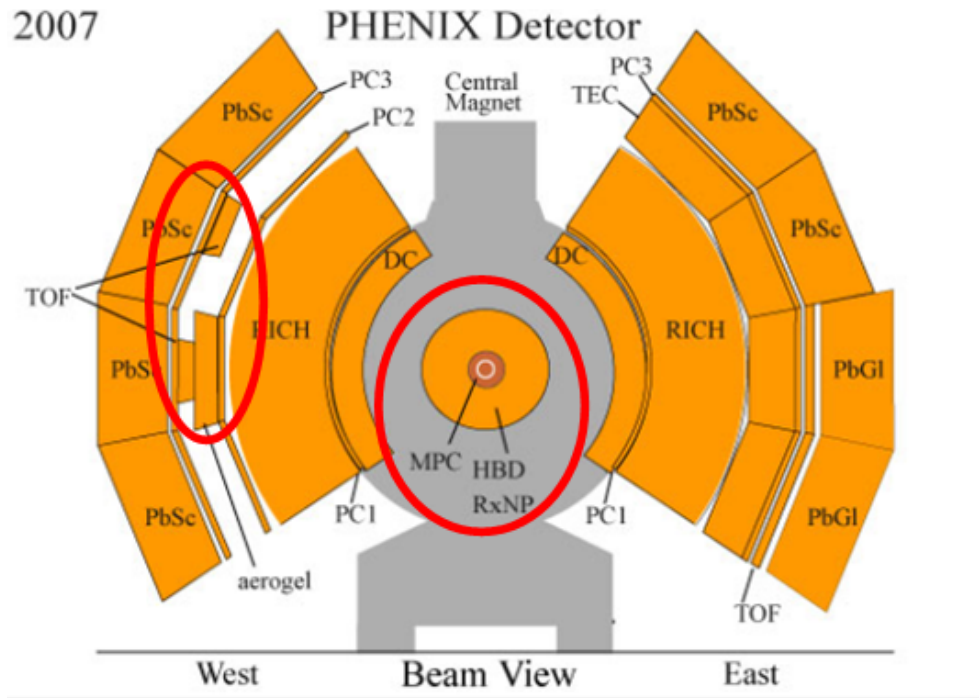


Figure 2: Configuration of PHENIX in Run-6, showing the location of the Reaction Plane Detector (RXNP), Time of Flight-West (TOF-W), Hadron Blind Detector (HBD) and the Muon Piston Calorimeter (MPC).

The Time of Flight -West is a multigap Resistive Plate Chamber covering $\pi/8$ in azimuth and $|\eta| \leq 0.35$ in pseudorapidity. It is located in the PHENIX West spectrometer arm. When combined with the existing Aerogel Cherenkov counter the TOF-W allows for K identification out to p_T of 4 GeV/c and separation of protons from mesons to $p_T \approx 7$ GeV/c. Measurements after installation into PHENIX show that the subsystem has an intrinsic timing resolution of 75 ps. The TOF-W has enabled PHENIX to extend our identified particle spectra to higher p_T , which in turn allows for new physics results from Run-7 Au+Au data on identified particle v_2, v_4 and R_{AA} .

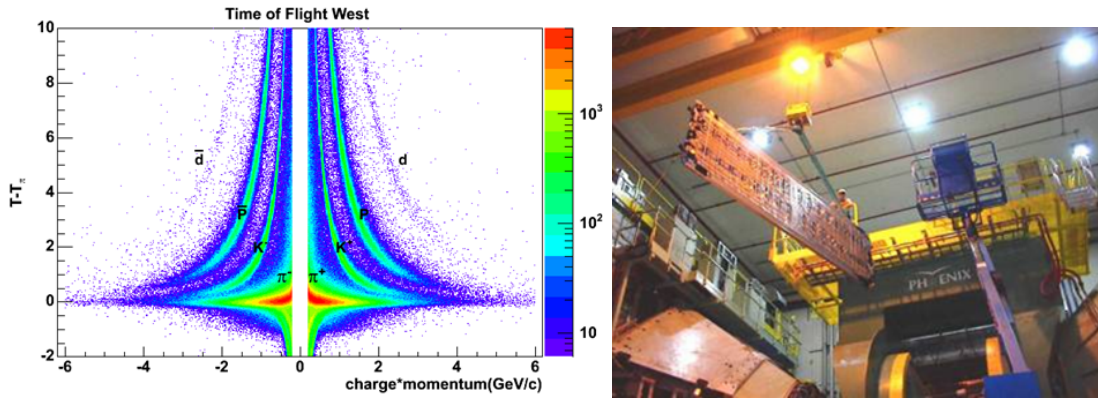


Figure 3: Left-hand: The time-of-flight versus charge times momentum measured by TOF-W in Run-7. Right-hand photo: Installation of the TOF-W into PHENIX in July, 2006.

The Reaction Plane Detector (RXNP) is composed of two arrays of scintillators segmented in both ϕ and η , covering pseudorapidity $1.0 < \eta < 2.8$ and 2π in azimuth. The RXNP arrays are mounted on the pole faces of the central magnet, as shown on the right side of Figure 4. As seen in the left side of Figure 4, the RXNP detector improves the accuracy of the reaction plane measurement by approximately a factor of two and allows for significantly more sensitive measurements of the collective flow via extraction of v_2 and v_4 . Note that here a larger value indicates better resolution. Additionally, the RXNP's resolution, when combined with the Aerogel and TOF-W detectors, enables determination of v_2 and v_4 for identified particles over a large range in p_T . This is illustrated by the left side of Figure 5. The right side illustrates how the higher statistics of Run-7, together with improved reaction plane resolution from the RXNP detector, results in a significantly improved heavy quark flow signal for $p_T \geq 3.0$ GeV/c. In fact, the new data show that the heavy quark flow continues to at least 5 GeV/c, where the contribution of single electrons from B meson decays should become significant. This is quite surprising and has already sparked considerable theoretical study.

The Muon Piston Calorimeter consists of two arrays of PbWO_4 crystals, covering 2π in azimuth and pseudorapidity $3.1 < \eta < 3.8$. Each MPC is located in front of a PHENIX forward muon spectrometer arm, as seen on the right side of Figure 6. Their purpose is to measure A_N and A_{LL} over a broad x range in polarized proton collisions; a preliminary result on A_N in 62.4 GeV p+p collisions is shown on the left side of Figure 6. Data from the MPC is also critical for studies of gluon saturation effects and the search for signatures of color glass condensate in d+Au and p+Au reactions. The MPC also contributes to the reaction plane measurements when combined with information from the Beam Beam Counters (BBC) and RXNP detector in heavy ion collisions. The MPC-South array was installed and commissioned prior to the Run-6 p+p run. The MPC-North array was installed prior to Run-7 and took Au+Au, d+Au and p+p data along with MPC-South

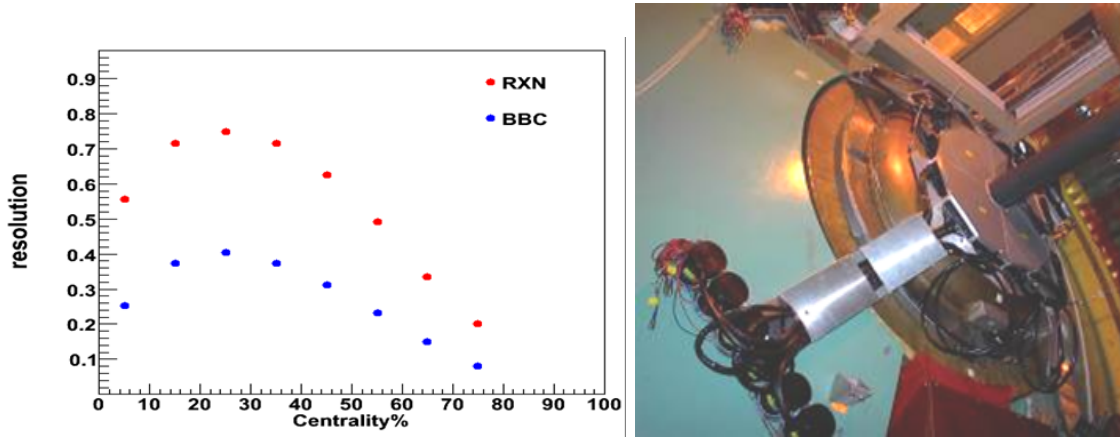


Figure 4: Left-hand figure: The RXNP detector improves the reaction plane resolution from 40% using the BBC to 74% at mid-centrality. Combining reaction plane measurements from the RXNP, BBC and MPC result in an event by event reaction plane resolution of 80%. Right-hand photo: b) One side of the RXNP detector installed on PHENIX magnet pole tip.

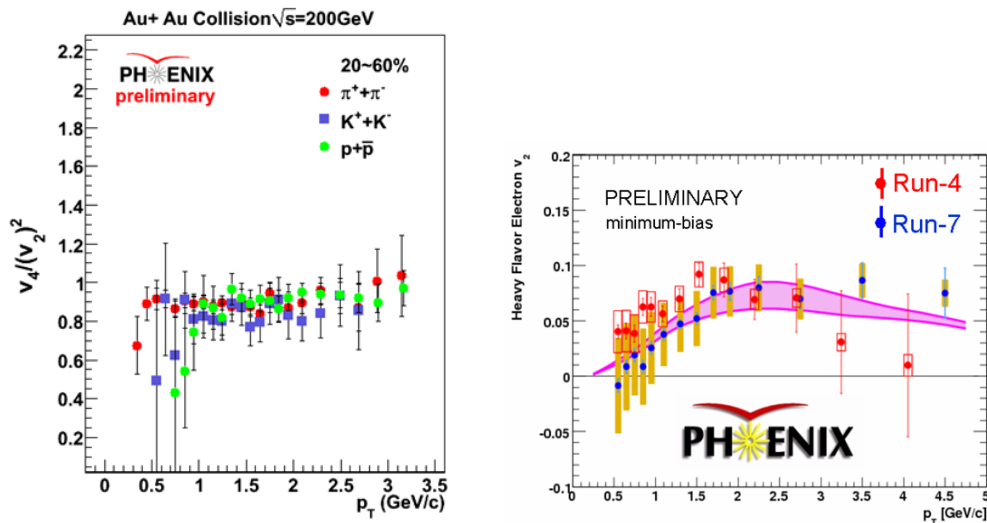


Figure 5: Left-hand figure: Identified hadron v_2 and v_4 measurements vs p_T in mid-central collisions. Right-hand photo: b) v_2 of non-photonic electrons; the dominant source of such electrons is the decay of D and B mesons. The blue points indicate the Run-7 data, and show that substantial elliptic flow is observed even for heavy quarks.

in Runs 7 and 8.

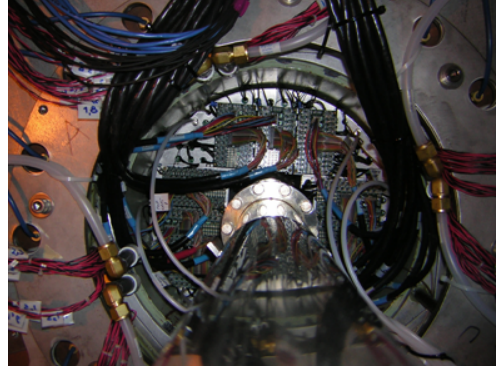
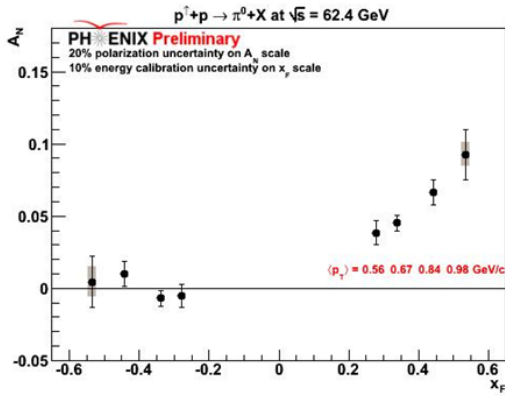


Figure 6: Left-hand figure: A_N as a function of x_F measured by the MPC-South detector in 62.4 GeV p+p data taken during Run-6. Right-hand photo: MPC-North Calorimeter installed in PHENIX.

3.3 Hadron Blind Detector

The Hadron Blind Detector (HBD) is a novel type of proximity focused Cerenkov detector, designed to be insensitive to the vast majority of charged hadrons created in the central rapidity region. The HBD's novel readout technology utilizes a stack of three GEM detectors with a CsI photocathode deposited on the top GEM. Essentially all electrons from external and internal conversions are detected, allowing rejection of the majority of pairs that form the combinatoric background in analyses of low-mass e^+e^- pairs. Reduction of this background is of crucial importance in this sector in which the signal pairs are sensitive probes of thermal radiation, chiral symmetry restoration and medium modifications to hadron properties. Results from Run-4 indicate an excess of low mass di-electrons in central Au+Au collisions, but are limited in both statistics and systematics by the very small signal-to-background ratio. The background rejection provided by the HBD is essential to obtain quantitative results.

3.3.1 HBD Commissioning in Run-7

Run-7 was the first run in which the HBD was installed, and served as an engineering run for this new detector system. An unexpected high voltage problem prevented raising the HV on the GEMs to normal levels, and resulted in excessive discharges that damaged a considerable fraction of the GEMs. This damage was exacerbated by a flaw in the firmware of the LeCroy High Voltage modules (1471N), which causes them to briefly re-assert voltage to the GEMs several hundred milliseconds following a discharge. Several weeks after the beginning of Run-7, one of the two arms of the detector (west) was dismantled to diagnose the problem. The east arm was operated for the duration of the

run, though not under optimal conditions.

The readout chain worked reliably and smoothly during the whole Run-7. The electronic noise was measured to be excellent *in all modules* with a typical σ value of 1.5 ADC counts. This corresponds to 0.15 fC or 0.2 p.e. at a gain of 5000. Other than the high voltage, all services and monitoring systems worked smoothly, in particular the recirculating CF_4 gas system and the monochromator system monitoring the gas transparency.

We now understand the origin of, and have solved, the HV problem encountered in Run-7. In the HBD stack assembly procedure, the GEMs easily hold now a ΔV of 511 V in CF_4 , typically yielding a gain of 20-30,000 on a triple GEM stack. This is well in excess of the normal operations with a gain of 5,000. We have considerably improved the protection against discharges by modifying the resistive chain powering scheme (some of these modifications were implemented already during Run-7) as well as the HV power supplies. The changes minimize the chance of damage when occasional discharges occur, and prevent involuntary reapplication of power after discharge.

The damaged GEMs have been replaced in the west arm. A large fraction were successfully recuperated by washing with deionized water, which is a routine operation at the end of the regular production of GEM foils. The west arm is fully refurbished and is presently undergoing tests. We are on track for installation of the entire HBD well before the start of run-9.

3.3.2 HBD Performance in Run-7

In spite of the far from optimal operational conditions of the east arm of the HBD in Run-7, the data collected are very useful to study the detector performance and demonstrate its capability to reject combinatorial background from photon conversions and π^0 Dalitz decays in the measurement of low-mass electron pairs. Figure 7 shows the distribution of residuals from matching electron tracks measured and identified in the central arms to hits in the HBD along z (the beam axis) and ϕ (azimuthal angle). The matching resolution both in z and ϕ is $\sigma_z \approx \sigma_\phi \approx 1$ cm, which is determined by the HBD hexagonal pads of size $a = 1.55$ cm ($2a/\sqrt{12} = 0.9$ cm).

The hadron blindness properties of the HBD are illustrated in Figure 8. The left panel demonstrates the suppression of the hadron response of the detector in reverse bias mode as compared to the forward bias case. The middle panel shows the electron-hadron separation in reverse bias mode. Adequate hadron rejection is achieved with a simple amplitude cut, as shown on the right panel. Hadron rejection factors in excess of 100 are obtained by combining the the amplitude cut with a cluster size cut, since hadrons produce single pad clusters whereas single electrons typically produce clusters of 2-3 pads.

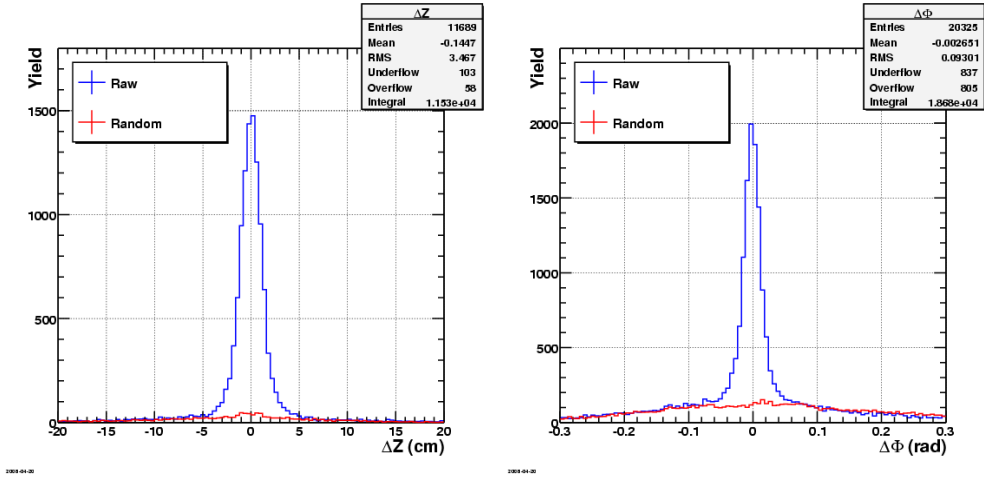


Figure 7: Matching distributions in z (left panel) and ϕ (right panel) of central arm tracks matched to the HBD.

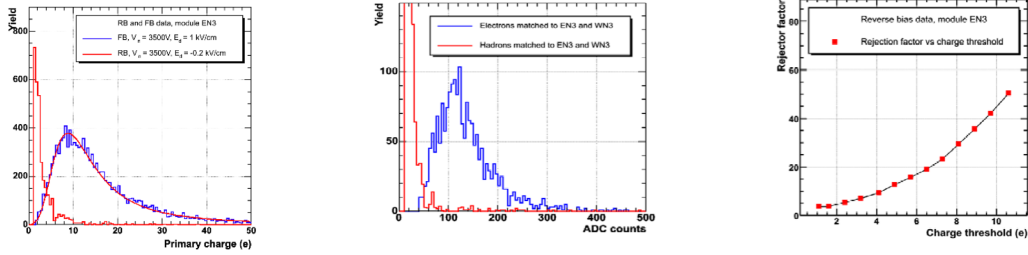


Figure 8: Left panel: hadron suppression illustrated by comparing hadron spectra in forward bias (FB in blue) and reverse bias (RB in red). Middle panel: electron-hadron separation in RB. Right panel: hadron rejection factor as function of the cut on the charge signal.

A key function of the HBD is its ability to separate two close or overlapping electrons from a single electron hit. The performance achieved in Run-7 is illustrated in Figure 9. The left panel shows the HBD response to double electrons selected by electron pairs identified in the central arm with an invariant mass $m \leq 150 \text{ MeV}/c^2$, where both tracks are matched to the same HBD cluster. The right panel shows the response to single electrons selected by electron pairs identified in the central arm with an invariant mass $m \leq 150 \text{ MeV}/c^2$, where the two tracks are matched to separate HBD clusters. The peak of the single electron distribution corresponds to ≈ 14 photoelectrons. This is low compared to the theoretical limit of 36 p.e. but not so far off when one considers known losses, including pad threshold: 10%, non-optimized reverse bias: 15-20%, and gas transmission losses of 15%.

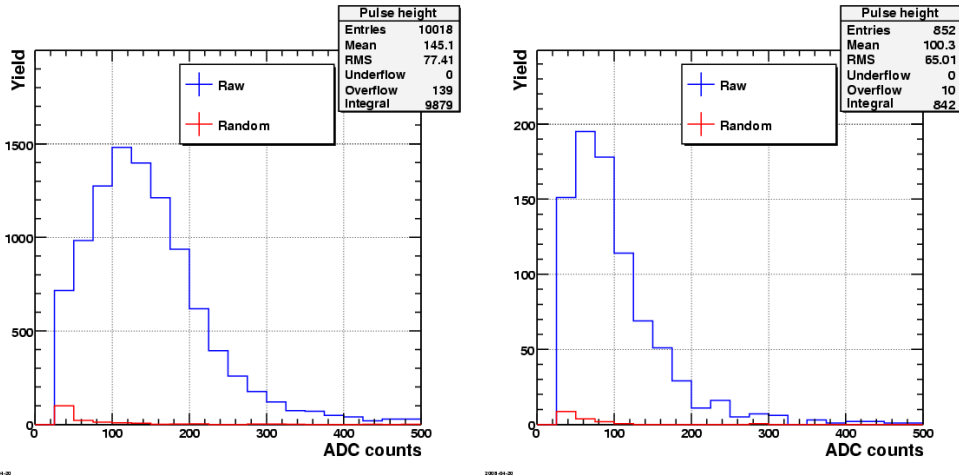


Figure 9: HBD response to double electron hits (left panel) and single electron hits (right panel).

	$m < 0.15 \text{ GeV}/c^2$		$m > 0.15 \text{ GeV}/c^2$	
	S	S/B	S	S/B
Before HBD rejection:	570 ± 88	0.16	31430 ± 187	17.1
After matching to HBD:	197 ± 34	0.41	14590 ± 123	53.3
Amplitude cut to reject doubles:	144 ± 22	0.81	14465 ± 121	145.2
Partial rejection of conversions in CF_4 :	175 ± 21	1.42	14464 ± 121	211.0

Table 2: Yield in the low and high mass regions as function of the rejection cuts.

The left panel in Figure 10 shows the invariant mass spectrum in the PHENIX east central arm, within the same acceptance of the HBD east that was operational in Run-7. This is the spectrum prior to any rejection of the combinatorial background using HBD information. The middle panel shows the same spectrum after applying HBD rejection utilizing the cuts described above. In both panels the red points represent the measured unlike sign spectrum and the blue points show the properly normalized combinatorial background determined by a mixed event technique. The right panel shows the net signal (unlike spectrum - combinatorial background) after HBD background rejection cuts. This is an ongoing analysis based on less than 10% of the available statistics and restricted to events with centrality $< 50\%$. The present results include only the HBD benefits from matching, double hit rejection and partial rejection of conversions in the radiator gas. The close hit cut and the cluster size cut are under investigation and not yet applied. Monte Carlo studies indicate that the latter two should further improve the combinatorial rejection power of the HBD. Even with this incomplete analysis the benefit of the HBD is apparent. The signal, as monitored by the π^0 Dalitz yield (with $m < 150 \text{ MeV}/c^2$), remains basically unchanged, whereas the combinatorial background is considerably reduced, resulting in an improvement of the S/B ratio by almost an order of magnitude for masses with $m > 150 \text{ MeV}/c^2$.

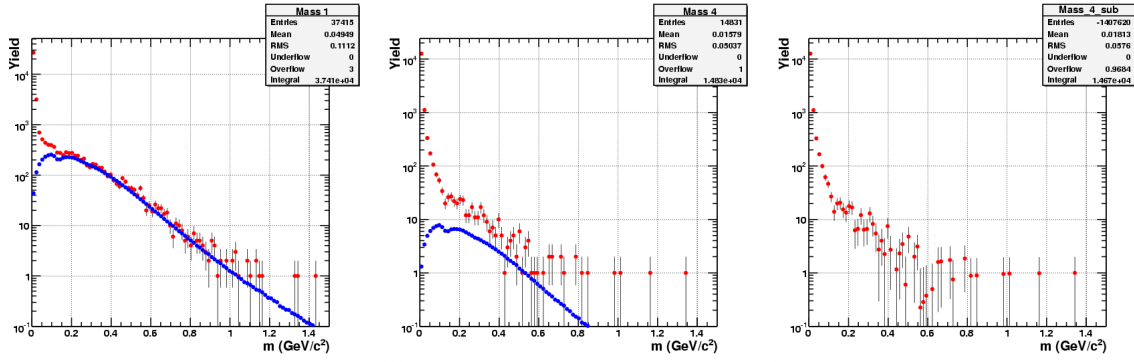


Figure 10: Invariant mass spectra before (left panel) and after partial (middle panel) background rejection cuts on HBD data. The red points represent the measured unlike sign pairs (U) and blue points the properly normalized combinatorial background (B) derived from a mixed event technique. The signal, obtained from the subtraction $U - B$ after HBD rejection cuts, is shown in the right panel.

The signal $S = U - B$ and the S/B ratio are quoted in Table 2 for the low ($m < 150$ MeV/ c^2) and high ($m > 150$ MeV/ c^2) mass regions as a function of the HBD cuts. The table shows that the HBD improves not only the statistical precision of the signal $S = U - B$ (through the reduction of the magnitude of both U and B) but also the systematic uncertainty. This is estimated to be approximately $0.25\%B$, and is improved via reduction of B. In the relatively low background of peripheral events selected in the present analysis, only the improvement in the statistical accuracy is shown in Table 2; the improvement in the systematic uncertainty is not yet apparent. This analysis is ongoing to include the full statistics of run 7, exploit the other information from the HBD that is not yet incorporated, and extend the analysis techniques to cope with the more central Au+Au events.

3.4 Future Upgrades for Installation Beyond Run-9

The PHENIX Beam Use Proposal is guided by the carefully structured, ongoing program of upgrades. In particular, the request is predicated on making all necessary measurements in Au+Au with the HBD in Run-9. Following that, the HBD will be removed from its data-taking position (along with the RXNP) in order to install the VTX detector, together with mechanical infrastructure to support the FVTX. Our requested Au+Au and p+p runs at 200 GeV will also provide proton+proton baseline measurements for the HBD physics program.

A program of substantial upgrades to the PHENIX detector has been developed to measure key observables which are either inaccessible at RHIC to date, or have been

measured only with limited precision and kinematic reach. The Muon Trigger, silicon central barrel vertex detector (VTX) and forward vertex detector (FVTX) are currently under construction, while the Nose Cone Calorimeter (NCC) awaits its cost and schedule review and we anticipate construction start this fiscal year. These major upgrades address observables that are critical to advancing understanding in three physics areas accessible at RHIC: high temperature QCD via the heavy ion program, the spin structure of the nucleon, and, thirdly, the parton content of the nucleus, which can be determined in "nucleon"-nucleus collisions.

3.4.1 VTX and FVTX

Precision tracking near the interaction vertex with highly segmented silicon detectors (VTX and FVTX) is being constructed to tag products from weak decays of mesons carrying heavy quarks (charm and bottom). The primary goal is to improve the signal to background on these measurements, and allow separation of charm and bottom. The silicon detectors will be used in conjunction with the electron tracks in the central arms and muon tracks in the muon arms to measure displaced vertices and tag the leptons from heavy meson semi-leptonic decays. The silicon detectors also will provide the mass resolution required to study the fate of different quarkonia in the partonic matter. The J/ψ measurements will be supplemented by ψ' and χ_C to probe the extent of color screening in the medium formed at RHIC. It should be noted that the VTX, having full azimuthal acceptance, and covering a pseudorapidity range larger than the PHENIX central arms, substantially increases the PHENIX acceptance for hadrons at midrapidity. Consequently, the VTX will improve jet correlations measurements of various types.

First measurements at RHIC with "non-photonic" leptons show that medium effects are large and heavy flavor seems to equilibrate more rapidly than expected. This calls into question our understanding of the energy loss mechanism in the dense, hot medium created in Au-Au collisions at RHIC, particularly the role of collisional energy loss. More detailed experimental data, particularly the fate of bottom quarks, are needed. Furthermore, these new detector systems will allow PHENIX to test predictions of recent theoretical work utilizing the duality between gravity and QCD-like field theory known as AdS/CFT correspondence. These calculations[25] show how measurements of heavy flavor energy loss and flow can be used to constrain fundamental parameters like diffusion lengths or viscosity of the medium. The ratio of charm to bottom suppression can show whether perturbative QCD or AdS/CFT provide more appropriate descriptions of the energy loss mechanism[26]. In addition, heavy flavor measurements add a new channel sensitive to gluon spin contributions to the elusive spin of the proton.

The VTX is supported by both the US (DOE) and Japanese funding agencies. The inner two layers of the VTX are two planes of pixel detectors, similar to those developed in the ALICE experiment at LHC. These inner planes will be ready for installation into

PHENIX in summer 2009, i.e. prior to run 10. The HBD and VTX/FVTX detectors are all located in the PHENIX central region inside the central magnet. Their installation and operation are tightly interlinked; in particular, it is not possible for the HBD and the silicon detectors to co-exist inside PHENIX. As discussed in detail above, the HBD is expected to operate successfully in the upcoming Run-9, and provide rejection of combinatorial background to allow precision measurement of the surprisingly large low mass dilepton excess at RHIC. We plan to use Run-10 as an engineering run for the VTX detector, operating the two pixel layers in the PHENIX environment, and making first measurements linking VTX pixel data with electron tracks measured in the central arms. In summer 2010 the full central barrel VTX detector (VTX) will be completed and installed into PHENIX. Consequently, we request full energy Au+Au collisions to utilize the VTX in Run-11.

Clearly, optimizing the PHENIX physics program in the next several years depends on the actual running time in 2009 and 2010. While the VTX will certainly be in place after Run-10, a Au+Au run in Run-9 sufficient to complete the HBD physics program would allow installation of the inner VTX layers for Run-10. This would provide for first data with the VTX prior to the first required physics production run; successful operation in Run-10 would advance the heavy flavor program and have significant impact globally.

The FVTX forward silicon vertex detector endcaps are funded by the DOE, and construction is currently underway. The FVTX is a three-year construction project, so we anticipate that this new PHENIX subsystem will be fully installed in summer 2011. As with the VTX, a partial installation and engineering run may be possible a year earlier. As the FVTX produces physics impact by adding high resolution tracking points for muons ahead of the hadron absorber, it is utilized together with muon arm tracks. Consequently, as with the VTX, a partial installation and successful commissioning prior to the first full run offers an excellent possibility for first physics results.

3.4.2 NCC

Forward electromagnetic calorimetry in the form of a novel, compact tungsten nose cone calorimeter with silicon readout (NCC) will provide both photon and neutral pion measurements in the forward direction. This new detector will effectively increase the current PHENIX acceptance by a factor of 10, as well as provide data in a different kinematic range than currently available.

The increased photon acceptance brought by the NCC, in combination with the extended acceptance for charged particle tracks in the silicon vertex detectors, will allow much higher statistics measurements of photon-jet correlations. This is true also for associated hadrons measured - and identified - in the PHENIX central arms. In polarized p+p collisions the NCC will provide data in the direct photon channel with known kinematics

(at least in first order perturbation theory). For high temperature QCD study, the ability to measure high statistics, high precision, photon-jet correlations will provide sufficient kinematic reach to differentiate descriptions of the energy loss of high momentum partons traversing the medium. In addition, the NCC is key to measure the χ_C . PHENIX will reconstruct its decay channel to $J/\psi + \gamma$, reconstructing the J/ψ in the PHENIX muon arms and the photon in the NCC. This information is crucial to clarify the surprising level of J/ψ suppression observed at RHIC, and to determine the relation of the observed suppression to color screening.

The NCC construction still awaits final approval and an official construction start, which we expect to receive before the end of FY08. The NCC will be constructed over a three year period, thus installation should take place in summer 2012.

3.4.3 Muon Trigger

PHENIX is pursuing two upgrades to our muon system, to allow triggering on high momentum muons. This new trigger capability is needed for a robust measurement of W boson production and asymmetries in polarized proton collisions at 500 GeV \sqrt{s} . PHENIX is constructing new electronics to split and process signals from the existing muon tracking chamber, which will provide triggering information in time for inclusion in the first level trigger decision. The second trigger project is construction of large-scale resistive plate chambers to complement the existing muon tracking capability and add to the muon tracker-based trigger. These chambers provide additional points along the muon tracks, and fast readout to allow momentum calculation at the trigger level. These two upgrades provide complementary information on the muon's momentum, and enter the first level trigger in different ways. The new triggering capability will provide for accumulation of sufficient statistics for W-bosons decaying to muons. The data will offer a unique and clean measurement of the flavor dependence of the sea quark contribution to the proton's spin. As current results on the gluon polarization indicate surprisingly small polarization in the accessible kinematic range, the 500 GeV running is an important new corner-piece for solving the nucleon spin puzzle.

The muon trigger upgrades are funded by the NSF and Japanese funding agencies, and both projects are already well advanced. The production of new trigger electronics for the muon tracker is under way, with the first arm's worth of boards ready for installation prior to Run-9. RPC prototype construction and study is complete, and production start of the RPC's is imminent. The PHENIX Collaboration has worked out an installation plan for these large new chambers. In principle, installation of the upgrades in the muon arms of PHENIX are logistically unrelated to installations in the vertex region. However, since the available workforce and the shutdown periods are finite, careful coordination is required. In general, most installation steps for the muon trigger upgrades are very involved and demanding, requiring extended time periods. We plan to install all components over the

next 3-4 years, depending on the RHIC operation and shut-down schedule.

4 Discoveries and Future Goals of the Spin Program

4.1 Longitudinally polarized proton collisions at $\sqrt{s}=200$ GeV

Determination of the gluon spin contribution to the spin of the proton (ΔG) is a paramount goal of the RHIC spin program. Currently the highest sensitivity to ΔG in PHENIX is achieved from double helicity asymmetry (A_{LL}) in π^0 production in the PHENIX central arms. Run-6 preliminary data on $A_{LL}^{\pi^0}$ [20] is consistent with the calculated $A_{LL}^{\pi^0}(p_T)$ GRSV curves assuming zero or moderately negative ΔG (Figure 12). The GRSV-std curve corresponding to moderately positive ΔG (~ 0.4 at $Q^2=1$ GeV²) is rejected on the level more than $3\sigma_{exp}$ (though no theoretical uncertainties are included). Run-9 with 25 pb^{-1} recorded integrated luminosity and 60% average polarization will decrease the statistical uncertainties for $A_{LL}^{\pi^0}$ by a factor ~ 2.3 .

Figure 11 shows the expected statistical uncertainties for $A_{LL}^{\pi^0}$ in Run-9 along with the “GRSV-0” and “GRSV-std” calculations [21]. Fig. 12 demonstrates the sensitivity of these data to ΔG in the probed x-range for two assumptions for ΔG within the GRSV model. The red curve demonstrates the limited sensitivity of mid-rapidity inclusive π^0 data to negative ΔG . If ΔG is at least slightly positive the PHENIX Run-9 data will be able to considerably improve the ΔG constraint, as illustrated by the blue curve, which assumes that ΔG is a half of the one corresponding to “GRSV-std”. We note that this is still consistent with our $A_{LL}^{\pi^0}(p_T)$ Run-6 preliminary data on the level $< 2\sigma_{exp}$.

Recently DeFlorian, Sassot, Stratmann and Vogelsang (DSSV) carried out a global QCD analysis of the available data sets of longitudinal double spin asymmetries obtained in deep inelastic scattering and from polarized proton-proton scattering experiments at RHIC [22]. All polarized data sets for which the perturbative QCD analysis framework used by the authors was able to quantitatively describe the associated unpolarized observable were included. From RHIC the DSSV analysis includes asymmetries observed in STAR in inclusive jet production and asymmetries for neutral pions measured in PHENIX. For the first time, the DSSV global QCD analysis makes it possible to demonstrate the impact of the RHIC data on the overall knowledge of $\Delta g(x)$. The analysis makes it further possible to estimate the global impact of 10 weeks of polarized p+p collisions at 200 GeV in RHIC Run-9; this study assumed an integrated luminosity of $\int L dt = 25 \text{ pb}^{-1}$ and a proton beam polarization of $P = 0.65$. The authors conclude that RHIC data constrain $\Delta g(x)$ strongly in the region $0.05 < x < 0.2$. Figure 13 compares the present best fit using RHIC Run-6 data with a fit using a projected Run-9 data sample from RHIC.

It is interesting to observe that the presently favored gluon distribution has a node

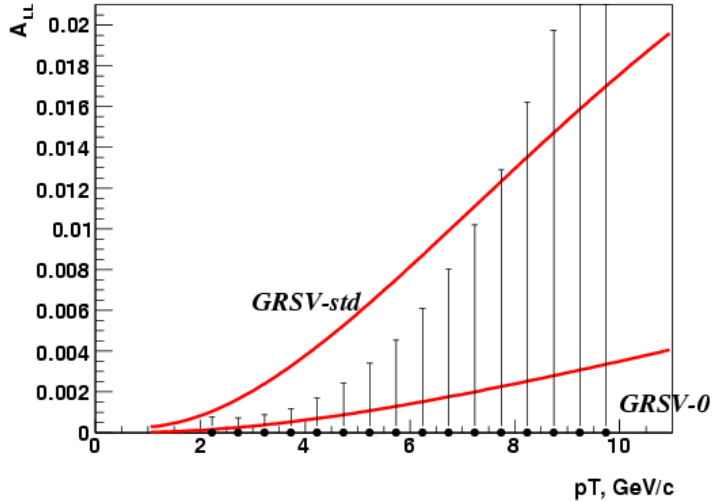


Figure 11: Projected $A_{LL}^{\pi^0}$ uncertainties in Run-9 along with calculations “GRSV-std” and “GRSV-0”.

at $x \approx 0.1$. The inclusion of Run-9 data will decrease the uncertainties in $\Delta g(x)$ very significantly. Quantitatively, this is illustrated by the authors with the help of curves showing the change in χ^2 from their global QCD fits as a function of the first moment $\Delta g^{1,[0.05-0.2]} = \int_{0.05}^{0.2} \Delta g(x) dx$. The χ^2 -distributions are shown in Figure 14. The authors carry out QCD fits using all the available data and subsets: DIS data only (red), semi-inclusive DIS only (yellow), STAR (jets) only (blue), PHENIX (neutral pions) (green) only. At the level of precision from the Run-6 data sample, it can be seen that $\Delta g^{1,[0.05-0.2]}$ is bounded on the positive side by DIS and PHENIX data and on the negative side by the STAR data. Inclusion of a hypothetical Run-9 data sample leads to much improved sensitivity dominated by the information from RHIC. For negative $\Delta g^{1,[0.05-0.2]}$ the A_{LL}^{jet} from STAR will provide the most sensitive constraint and for positive $\Delta g^{1,[0.05-0.2]}$ the PHENIX $A_{LL}^{\pi^0}$ will provide the best determination.

The Run-9 projected luminosity and polarization will allow, for the first time, to include other measurements in the global fit of ΔG . The other observables, e.g. charged pions, η , charm, etc. will provide multiple handles on the determination of the polarized gluon distribution. Figures 15 and 16 show the expected statistical uncertainties for charged pion A_{LL} in Run-9 along with the “GRSV-0” and “GRSV-std” calculations. The expected sensitivities are sufficient to distinguish the ΔG assumed in “GRSV-std” from “GRSV-0”. The quark-gluon subprocess starts to dominate for pion production at $p_T > 5$ GeV/c, leading to approximately linear dependence of the asymmetries on ΔG . The preferred fragmentation of π^+ from an up quark and π^- from a down quark and the fact that Δu and Δd have opposite signs lead to an ordering of the pion asymmetries depending on the sign of ΔG . Thus charged pion A_{LL} measurements at high p_T will

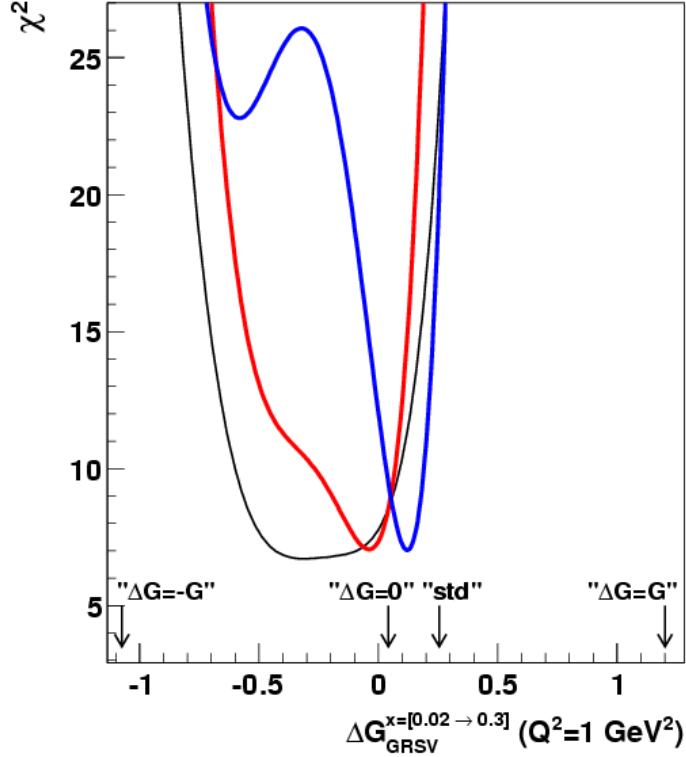


Figure 12: The χ^2 distribution of the data plotted versus the value of the first moment of the polarized gluon distribution in the x_g range from 0.02 to 0.3 corresponding to our π^0 data in p_T bins from 2 to 9 GeV/c. Black: Run6 preliminary data; red: Run9 projected data assuming “GRSV-0” model for ΔG ; blue: Run9 projected data assuming (“GRSV-0” + “GRSV-std”)/2 model for ΔG ($\Delta G \sim \Delta G^{GRSV-std}/2$). Only statistical uncertainties were used for each curve. Arrows indicate ΔG corresponding to the different polarized gluon distributions from GRSV calculations.

provide enhanced sensitivity to the sign of ΔG compared to neutral pions alone.”

Measurement of the direct photon asymmetry will give an independent determination of ΔG . In direct photon production the gluon Compton process ($qg \rightarrow q\gamma$) is dominant, so the double helicity asymmetry will be linear with gluon polarization. Consequently, PHENIX will be able to measure both the sign and value of ΔG through this channel. The expected sensitivities for direct photon A_{LL} from Run9 will, however, still be below the level required to constrain ΔG ; an additional factor of 2–3 is required, given that our Run6 π^0 data already indicate that ΔG is not large in the probed x -range.

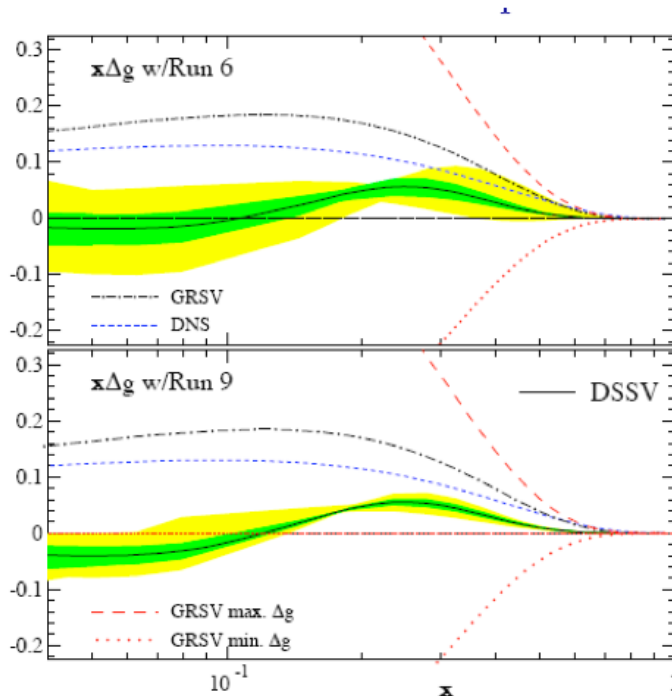


Figure 13: Best DSSV fits for the spin dependent gluon distribution $x\Delta g(x)$ including uncertainty bands. Top: all present data (DIS, SIDIS, pp). (bottom): all present data + projected RHIC results from Run-9.

4.2 Longitudinally polarized proton collisions at $\sqrt{s}=500$ GeV

Another principal goal of the RHIC Spin program is to measure anti-quark and quark polarization identified by flavor using the parity-violating production of W bosons, identified through high p_T leptons, typically at $p_T > 20$ GeV/c.

Almost direct quark/anti-quark separation is possible with forward/backward W production in PHENIX muon arms due to much larger quark density vs anti-quark density at large momentum transfer. In this case, $A_L(\text{forward } W^+) \approx \Delta u/u$. Similarly, $A_L(\text{backward } W^+) \approx \Delta \bar{d}/\bar{d}$. The parity-violating asymmetry of W^+ production in central rapidity combines contributions from both u and \bar{d} polarizations. Additionally, measurement of W^- production will give access to $\Delta d/d$ and $\Delta \bar{u}/\bar{u}$.

Figure 17 shows the relative yield for W production as well as for charged pions, the main high p_T background for W measurements. Our study several years ago demonstrated that the hadronic background can be considerably suppressed, by up to a factor of 1000:

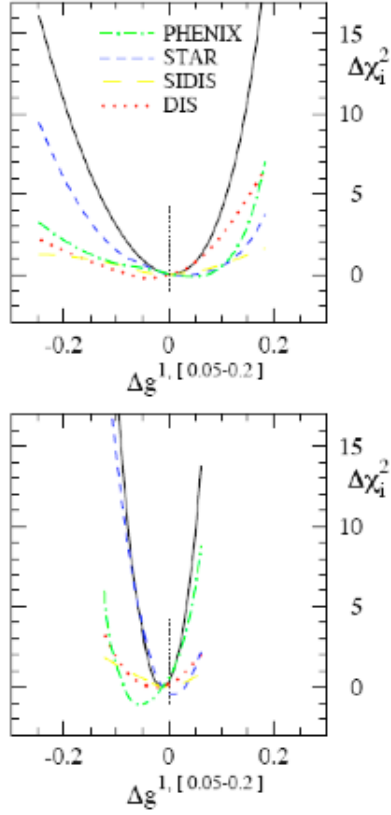


Figure 14: Constraints for $g^{1,[0.05-0.2]}$ with present data (top) and including the Run-9 projected data (bottom). The constraints are also shown for individual data sets.

- E/p matching (comparison of track momentum with EMCAL cluster energy), factor 25;
- Electromagnetic shower profile in the EMCAL, factor 10;
- Isolation cut, factor 5.

In Run-9, we will perform first tests of the new muon trigger electronics, and explore the background to high p_T tracks in the muon arms. With 25 pb^{-1} recorded integrated luminosity we expect to record ~ 500 (90) of W^+ (W^-) in the PHENIX Central Arms. For polarization of 60%, this translates to a longitudinal single spin asymmetry (A_L) uncertainty of 0.05 for W^+ . This first run will allow detection of the parity violating

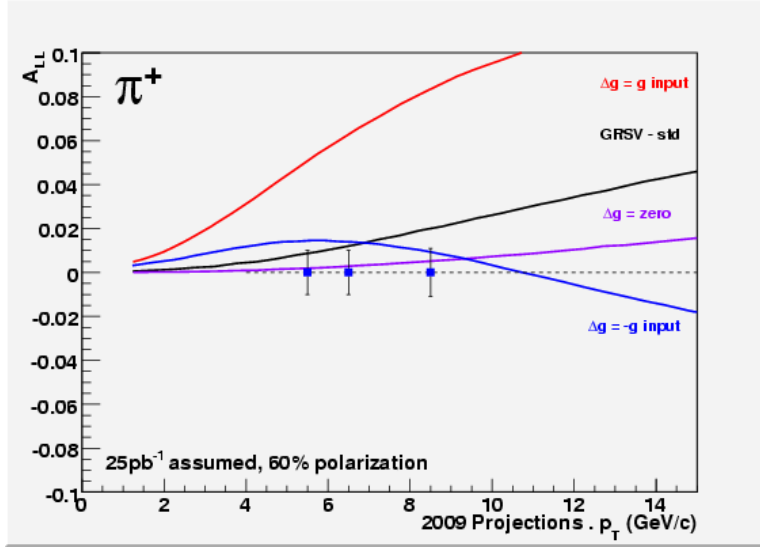


Figure 15: Projected $A_{LL}^{\pi^+}$ uncertainties in Run-9 along with GRSV calculations with different ΔG assumptions.

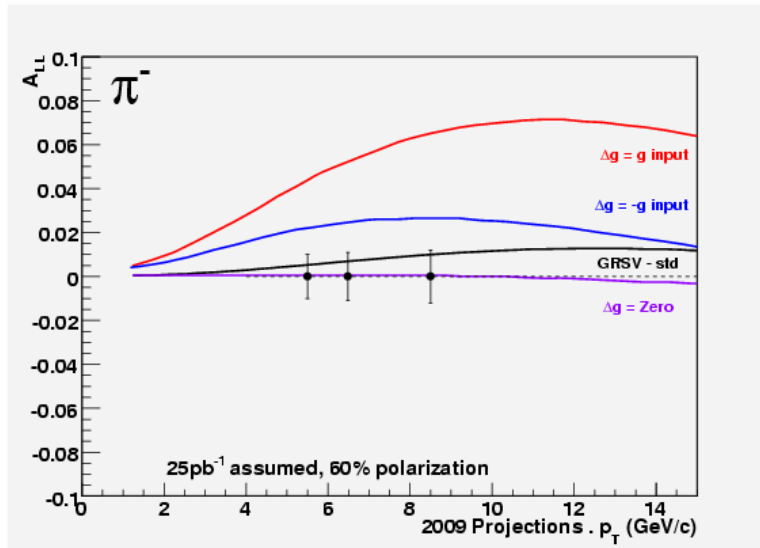


Figure 16: Projected $A_{LL}^{\pi^-}$ uncertainties in Run-9 along with GRSV calculations with different ΔG assumptions.

asymmetry on the level $> 5\sigma$, which is predicted by different calculations to be 0.25–0.40 for W^+ in the central rapidity region. The asymmetry is slightly smaller for W^- .

Furthermore, 25 pb^{-1} recorded integrated luminosity will allow measurement of unpolarized cross sections for different particle production, such as π^0 and prompt γ up to at least $p_T = 30 \text{ GeV}/c$. Several hundred thousand $J/\psi \rightarrow \mu^+\mu^-$ and a few hundred

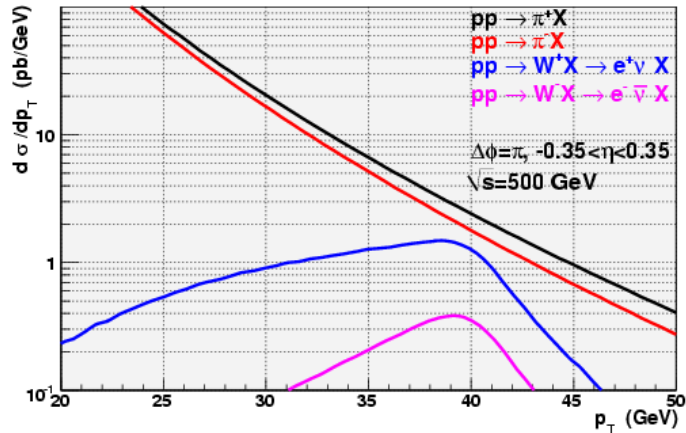


Figure 17: Simulated yield of electrons in the central arms from W decays, along with charged pions, which are the main source of high p_T background to W measurements.

$\Upsilon \rightarrow \mu^+ \mu^-$ are expected in PHENIX Muon Arms.

5 Discoveries and Future Goals of the Heavy Ion Program

Heavy ion collisions at RHIC have produced striking - and very surprising - results. A dense, hot, collectively flowing medium is created, which is extremely opaque to quarks and gluons traversing it. In our White Paper, PHENIX laid out the evidence that this medium is partonic, not hadronic, in nature[24]. Discoveries since that was published further strengthen this conclusion.

5.1 Opacity and Collective Flow

PHENIX has shown that even charm quarks are effectively stopped by the medium, and that they participate in the collective flow along with everything else[27]. We have made great strides in quantifying the energy loss by constraining various energy loss models with high quality data[16]. The outcome of these studies has sparked an enormous amount of theoretical work and debate in the field. It has proven difficult, though perhaps not impossible, to reproduce the observed light and heavy hadron suppression using perturbative descriptions of the energy loss. However the alternate extreme of very strong coupling is neither clearly required nor ruled out by the existing data. The role of collisional energy loss is under active study, and a unified picture that can describe the mass, centrality,

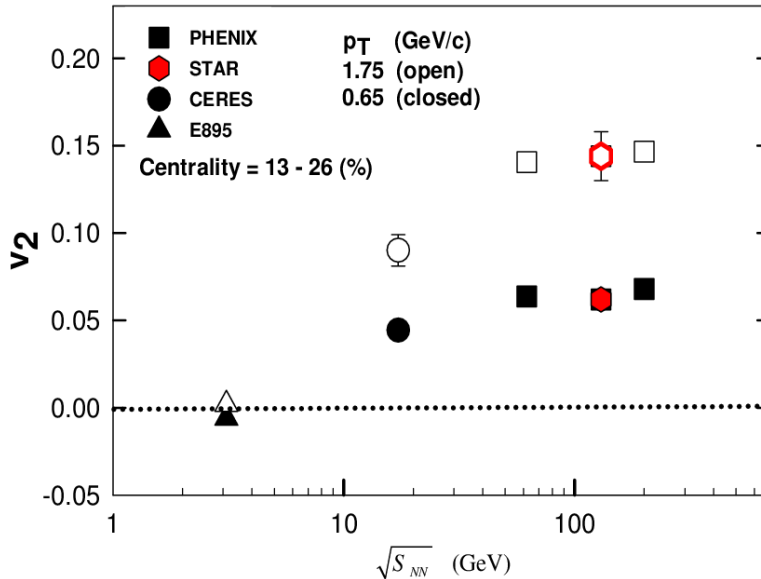


Figure 18: v_2 of charged hadrons at two values of p_T , as a function of $\sqrt{s_{NN}}$ [28]. Results are shown for collision centrality of 13% to 26%.

p_T , reaction plane, and beam energy dependence of parton energy loss has yet to be discovered. Progress on this question requires theoretical effort, but also high precision data on light hadron suppression at the highest p_T , the reaction plane dependence of energy loss, separate determination of charm and bottom energy loss, and direct photon-hadron correlation data to probe directly the medium effect upon fragmentation functions.

As shown in Figure 1, PHENIX has found that the medium becomes opaque to light partons at \sqrt{s} somewhere between 22.4 and 62.4 GeV in Cu+Cu collisions. Locating the onset would allow us to pinpoint the onset of the perfect fluid at RHIC and determine its other properties at the onset point. It is imperative to measure at the same time the elliptic flow of pions, kaons and protons to see whether v_2 saturation, shown to hold for high \sqrt{s} collisions in Figure 18, sets in at the same point. Below the critical point, the per quark scaling of v_2 may be broken, motivating study of baryon and meson flow separately. Careful comparison to viscous 3-d hydrodynamics calculations will allow extraction of the shear viscosity to entropy ratio, η/S to see whether it reaches a minimum, as is expected at the critical point, followed by a sharp increase as the collision energy is reduced further. Searching for the onset of opacity also requires baseline measurement of p+p collisions at the same \sqrt{s} .

A related goal is to determine experimentally whether the opacity to heavy quarks observed in 200 GeV Au+Au collisions sets in at the same point as opacity to light quarks. Answering this question requires measurement of non-photonic electron R_{AA} along with π^0 R_{AA} and v_2 of several additional species of identified hadrons. Preliminary PHENIX results for charm production via semi-leptonic decay to electrons, shown in Figure 19

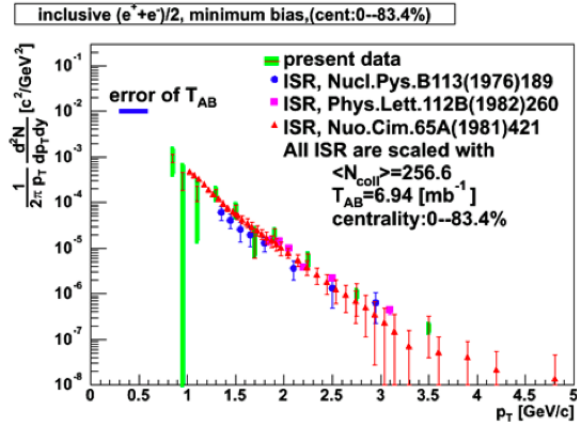


Figure 19: Spectrum of non-photonic electrons in minimum bias Au+Au collisions at 62.4 GeV, compared to p+p collisions at top ISR energy.

indicates that at 62.4 GeV, R_{AA} for charm is near 1, contrary to data at higher collision energy. This provides a first hint, albeit with large uncertainty, that the onset of opacity for charm quarks is at a higher \sqrt{s} than for light quarks.

PHENIX has made precision measurements of the bulk collective flow of many different hadrons, including those with heavy quarks. Quantitative comparison with hydrodynamic models provides evidence that the viscosity is extremely small, approaching the quantum limit of minimal viscosity. This is the basis of the conclusion that matter produced at RHIC is perhaps the most perfect fluid created in the laboratory.

PHENIX has taken the next step in experimental study of the viscosity. We use the energy loss and collective flow of charm quarks to provide constraints on the viscosity to entropy ratio η/S , independently of comparing light hadron flow to hydrodynamic calculations. The conclusions are limited by the statistical precision of the measurement of single electrons from non-photonic sources. As can be seen in the right panel of Figure 5 in the Run-7 section above, the improved reaction plane resolution of the RXNP detector and the higher statistics of Run-7 provide a substantial improvement upon the Run-4 result. Nevertheless, a substantially larger data set obtained by combining Run-7 and Run-9 is crucial to improve statistical and systematic uncertainties. Beginning in 2011, the VTX detector will provide charm and bottom separation, allowing PHENIX to determine whether bottom quarks also experience significant energy loss and drag in the produced medium; current expectations are for these very heavy quarks to be poorly stopped by the medium. The luminosity increase due to stochastic cooling, along with the new capabilities with vertex detectors, are key to addressing this.

5.2 Low Mass Dileptons and Thermal Radiation

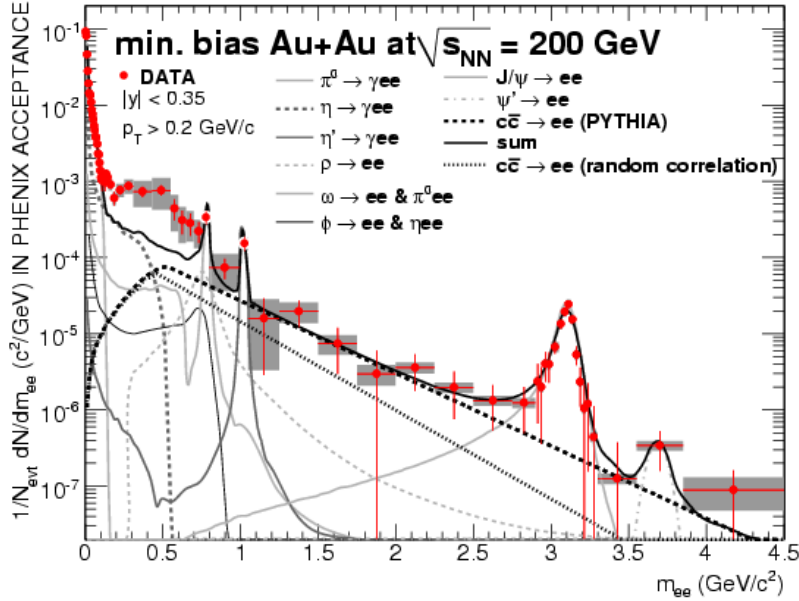


Figure 20: The Run-4 PHENIX minimum bias dielectron yield as a function of invariant mass. Vertical lines represent statistical errors and gray boxes represent systematic errors.

Di-electron measurements in Run-4 Au+Au and Run-5 p+p have shown remarkable features. A large excess is observed at small invariant mass; this is visible as a “bump” above the solid line indicating di-electrons from hadronic sources in Figure 20. No excess is observed in p+p collisions at the same energy. The excess in Au+Au exceeds that in lower energy collisions at CERN, and there is considerable discussion about its source. While the lower energy result is generally interpreted as a medium modification of the ρ meson spectral function, the hadron gas phase of the collision is usually expected to be less dominant at RHIC energy. The centrality and p_T dependence of the excess are under study, but the large combinatorial background causes substantial statistical uncertainties resulting from the subtraction of two large numbers. The systematic errors are large as well, due to uncertainties in normalization of the combinatorial background. Consequently, the Run-4 data lack the precision required for fine binning in mass, and provide for only limited sensitivity to expected modifications of spectral functions. Rather than a single bin at the ω peak, several-fold finer binning is needed. A four-fold improvement requires a data set with effectively 16 times more statistical and systematic precision. This will also allow us to quantify the centrality and p_T dependence of the excess.

At low mass and high p_T , di-electrons are produced by the same mechanism as direct photons. The p_T spectrum of di-electrons above 1 GeV/c p_T has a shape characteristic of a sum of pQCD direct photons at high p_T and direct photon “internal” conversions at moderate p_T . PHENIX has just submitted a paper analyzing the photons as emission

from a thermal source. An initial collision temperature in the range of approximately 300-500 MeV is inferred from the data. An enhanced data set will allow better precision on the temperature by better differentiating among models, and providing the centrality dependence of the initial temperature.

5.3 Color screening and quarkonia

PHENIX has shown that, as predicted, J/ψ are suppressed at RHIC. Surprisingly, though the suppression is not extremely different from that observed at the SPS at center of mass energy an order of magnitude lower. Furthermore, the suppression at forward rapidity is found to exceed that at midrapidity. As these results run counter to expectations from color screening in the medium, there is tremendous theoretical work ongoing to understand them. One possible explanation is that many of the observed J/ψ 's are not in fact primordial, but are regenerated by final state coalescence charm and anti-charm quarks which have been caught up and scrambled by the medium. This hypothesis can be checked by measuring the elliptic flow of the J/ψ , which requires a very substantial amount of data.

Other questions about quarkonia include the p_T dependence of the suppression for J/ψ and the magnitude of the suppression as a function of the binding energy, or size, of different quarkonium states. There are several predictions of the high p_T behavior of J/ψ suppression, with different theoretical descriptions predicting opposite trends. High quality measurement will sort these out.

5.4 Medium Response to deposited energy

Data on di-hadron and three-hadron correlations show remarkable modifications for intermediate energy particles. These effects are sometimes interpreted as evidence that the energy lost by traversing quarks and gluons shocks the medium it is deposited into. Indeed, some of the patterns resemble those in other shocked media. However, there remain considerable uncertainties both in the interpretation and in the data. Higher precision data are required to support or contradict the hypothesis of shocks. It will be important to see whether it is possible to differentiate strongly medium-modified jet fragmentation from the excitation of co-moving medium particles. The suppression pattern, and reaction plane dependence at high p_T provides an important baseline, but is currently statistically limited. More data are also required to quantify the associated particle spectra with direct photon triggered jets.

5.5 Search for the QCD Critical Point

As the results from RHIC indicate that the medium is partonic, rather than hadronic, mapping the QCD phase diagram is key to elucidating the nature of the phase transition. A major goal is to search for the critical point in the QCD phase diagram, where a first order phase transition between a hadron gas and quark gluon plasma (at low values of the baryon chemical potential, μ_B) turns into a more subtle "crossover." There have been several workshops around the world centered upon developing approaches for such a search. Theoretical expectations for the critical point suggest it will be found when the baryon chemical potential is in the range $150 < \mu_B < 500$ MeV. This corresponds to collision energies in the range $5 < \sqrt{s} < 30$ GeV. Rajagopal suggests that it is not necessary to be particularly close to the critical point to be sensitive to it, suggesting an energy scan in steps of 50-100 MeV in baryochemical potential. As this critical point must be related to the onset of the perfect liquid, it is natural to begin this search at the high energy (low baryochemical potential) end of Table 3, and work our way downward in energy, where RHIC operations become more challenging and luminosity much lower.

μ_B	$\sqrt{s_{NN}}$
550	5
470	6.3
410	7.6
380	8.8
300	12.3
220	18
150	28
75	60

Table 3: Relationship between baryon chemical potential and center of mass collision energy.

Many signatures have been proposed to help identify the approach to the critical point. The pion and non-photonic electron R_{AA} opacity observables and identified hadron v_2 were described above. A number of predicted critical point signatures involve non-statistical fluctuations in quantities such as event multiplicity, mean transverse momentum, K/π ratio, etc. Such fluctuations are expected as one approaches the critical point since assumptions about indistinguishability of individual events can be violated. Signatures such as non-monotonic behavior of the K/π ratio vs. energy have also been predicted, as have modifications to η/S , as determined from identified particle flow (v_2) measurements binned in centrality. Identified particle spectra are useful tools to characterize the hadron gas phase of the collision. From these, the freeze-out temperature and radial flow of the hadrons, which reflect the expansion velocity can be extracted.

In general, the field of heavy ions has found that the collisions are so complex, and the

theoretical models used to describe them are so tunable, that it is crucial to be able to collect enough data to allow a simultaneous exploration of a large number of signatures (two-particle Hanbury-Brown Twiss correlations, in-medium mass modifications, charmonia, etc.). Of course, the ability to measure any given signature decreases with energy as the particle yield per event decreases. This mandates collection of substantial numbers of events, as detailed below.

5.6 Heavy Ion Running Requirements

5.6.1 Completion of High Statistics Au+Au Data Set

We will search for evidence of heavy quark recombination to produce J/ψ at freezeout, which would mask suppression by the color screening early in the collision. This is accomplished by measuring the J/ψ elliptic flow. This requires completion of the order-of-magnitude larger Au+Au data set. Figure 21 shows a preliminary result from approximately half of the Run-7 data on $J/\psi \rightarrow e^+e^-$. Clearly the data as yet lack the required statistical precision. Figure 22 shows the quality of the measurement expected from a data set ten times that of Run-4 (i.e. Run-7 + $1.5 \times$ Run7).

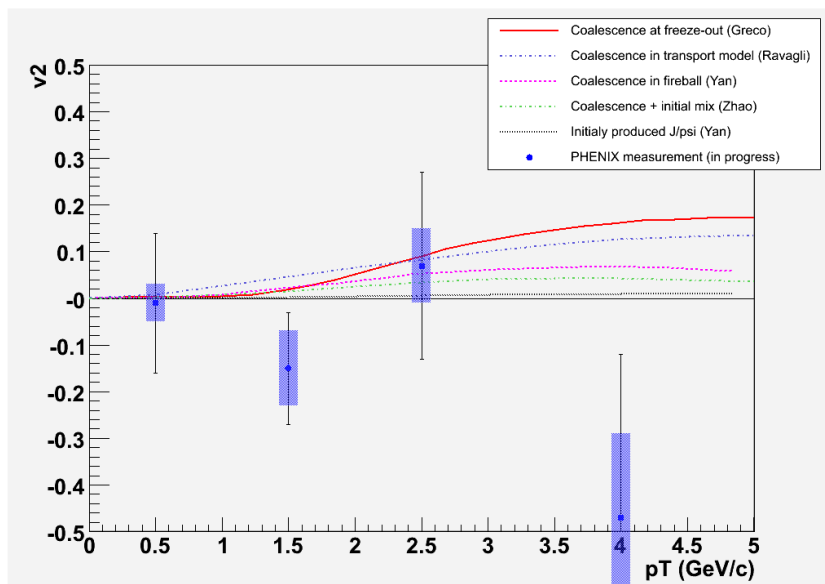


Figure 21: Preliminary analysis of Run-7 data on flow of J/ψ detected in the e^+e^- channel. The plot contains approximately half of the central arm data.

Similarly, investigation of direct photons at the highest p_T to see whether the apparent decrease of R_{AA} below one holds requires ten times Run-4 statistics, as do correlations of hadrons with direct photons. Currently we only have 4 times Run-4, and consequently

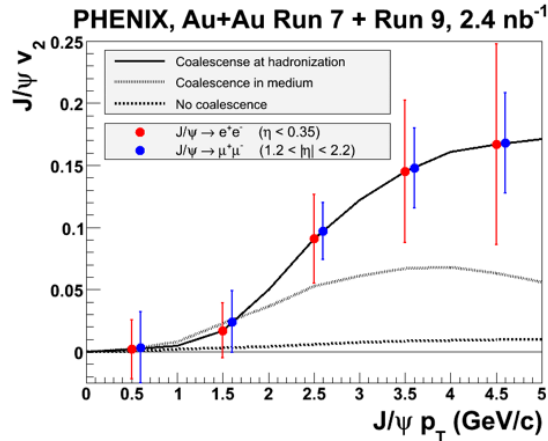


Figure 22: Projected sensitivity to $J/\psi v_2$ in Run=7 + Run-9 data combined.

need to record the remainder in Run-9. These are high impact observables for characterizing the medium. It is crucial to have the data prior to turn-on of LHC, in order to maintain high visibility of RHIC program and continue to provide exciting physics results.

5.6.2 Low Mass dileptons with HBD in Run-9

The effectiveness of the HBD in distinguishing closely separated electron pairs from isolated single electrons has been demonstrated as adequate from the Run-7 results. Improvements are expected in Run-9 due to increased light yield from better gas transparency ($\approx 15\%$ improvement). The voltage bias configuration ($\approx 10-15\%$ losses) will also be improved. Simulations of the HBD performance, tuned to bench tests from a scintillation light source, have been used to determine the improvement of the dielectron measurement as a function of the photo-electron yield in the HBD and the size of the data set.

Figure 20 shows that the existing results for low mass dielectrons are limited by systematic uncertainties[30]. These are dominated by the uncertainty in normalizing the large combinatorial background. The HBD will reduce this combinatorial background, thereby reducing both the systematic and statistical errors. To quantify the expected effect, we define an effective signal size, S_{eff} as the number of signal counts in a background-free measurement that would have the same relative error bar as our final measurement. We use this quantity in order to put together the various effects of the HBD. While rejection of double electrons in the HBD improves the background, placement of the single-double

cut also affects the efficiency of tagging single electrons (the signal). Furthermore, the HBD introduces material into the PHENIX acceptance and so produces an additional background. S_{eff} quantifies these competing effects, and allows comparison of the expected performance to that observed in PHENIX in Run-4 with no HBD. The expression below shows how this effective signal size depends upon the signal and background terms:

$$\frac{1}{\sqrt{S_{eff}}} = \frac{\sqrt{\sigma_{stat}^2 + \sigma_{sys}^2}}{S} = \frac{\sqrt{(\sqrt{S + BG})^2 + (BG \times \sqrt{\sigma_{LikeSign}^2 + (0.2\%)^2})^2}}{S}$$

Simulated signal and background were generated using an electron cocktail tuned to PHENIX measurements. The HBD performance was simulated for two extreme cases: (i) accounting only for HBD-based single-double separation, (ii) accounting for both single-double separation and increased purity of the electron sample due to additional electron-ID from the HBD. The Run-7 data analysis would indicate that the actual HBD performance lies between these two extremes.

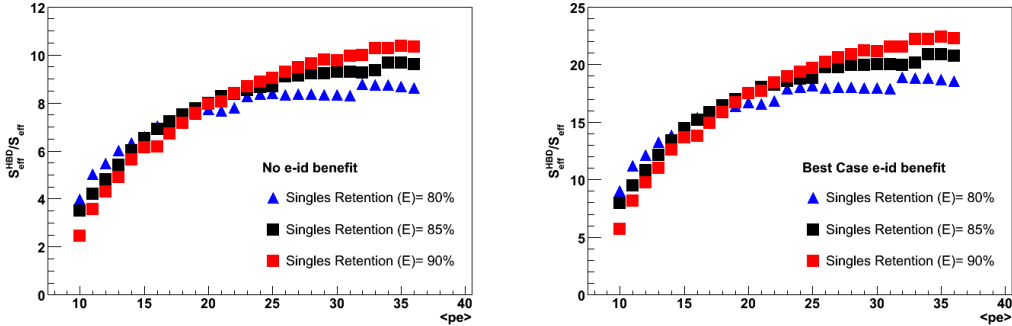


Figure 23: The ratio of the effective signal with the HBD over that without an HBD is shown as a function of the raw photo-electron yield. The left panel assumes no benefit from additional electron-ID using the HBD. The right panel assumes the theoretical maximum additional electron ID in the HBD. The different symbols show performance with different cuts to separate single from double electrons; the cut effect is quantified via the single electron signal retention performance. The HBD in Run-7 yielded 14 photo-electrons and electron identification performance in between these two extremes.

Figure 23 shows the ratio of effective signal with an HBD to that of baseline PHENIX without the HBD, as a function of the number of photoelectrons detected by the HBD. The effective signal calculated without and with accounting for HBD eID performance. The range of the plot extends from below the Run-7 result (14 photo-electrons) to the design performance (36 photo-electrons). The three curves on each side correspond to different cut values separating single from double electrons. They cross one another

because S_{eff} depends both on the signal level, S , and, with a different functional form, on the background level, BG . Figure 24 shows the ratio of the effective statistics of dielectrons in the low mass region as a function of the length of AuAu running time, f . Here f is the ratio of Run-9 integrated luminosity to that of Run-4. For a physics run collecting integrated luminosity comparable to that of Run-7 (i.e. 0.8 nb^{-1} recorded), the effective statistics of the low mass dielectron measurement would be increased by at least a factor of 16 over the existing Run-4 result. This estimate assumes no improvement in photoelectron performance and no benefit from electron ID in the HBD; with anticipated performance improvements the effective statistics ratio is likely to increase over Run-4 by a factor closer to 36. Thus, a Au+Au run approximately equivalent to Run-7 with the HBD in place would reduce the overall error of the dielectron measurements by a factor of 4-6. Such an improvement is the minimum required to allow for study of the mass, p_T , and centrality of the large low mass excess observed by PHENIX. Collecting this data set in Run-9 will allow the Collaboration to achieve the physics goals of the HBD and replace it with the VTX detector for open charm and bottom measurements beginning in Run-10.

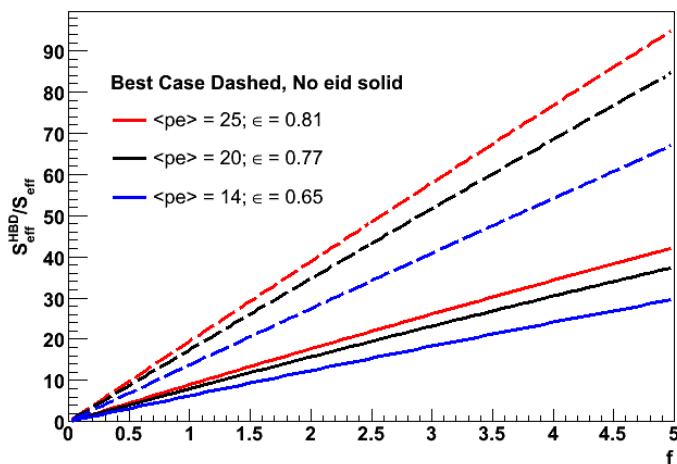


Figure 24: The effective signal relative to that in Run-4 is plotted as a function of the ratio of Run-9 integrated luminosity divided by Run-4 integrated luminosity.

Figure 25 shows the NA60 measurement of the spectral function of the ρ meson in central In+In collisions at $\sqrt{s} = 17 \text{ GeV}$ per nucleon pair[31]; $25 \text{ MeV}/c^2$ mass bins allow determination of the shape of the distribution. These data have been used to challenge many of the models of ρ in-medium broadening at the density and temperature achieved in full energy collisions at the SPS. It is imperative to constrain those explanations by comparison to broadening and possible mass shifts in the much hotter, initially partonic, medium at RHIC. This measurement is an essential ingredient to separating effects of the hot hadron gas from partonic effects at RHIC. Comparison of this plot to Figure 10 shows that such an analysis would be impossible in PHENIX without the background rejection from the HBD. However, with a factor of approximately 4 improvement in total error, the

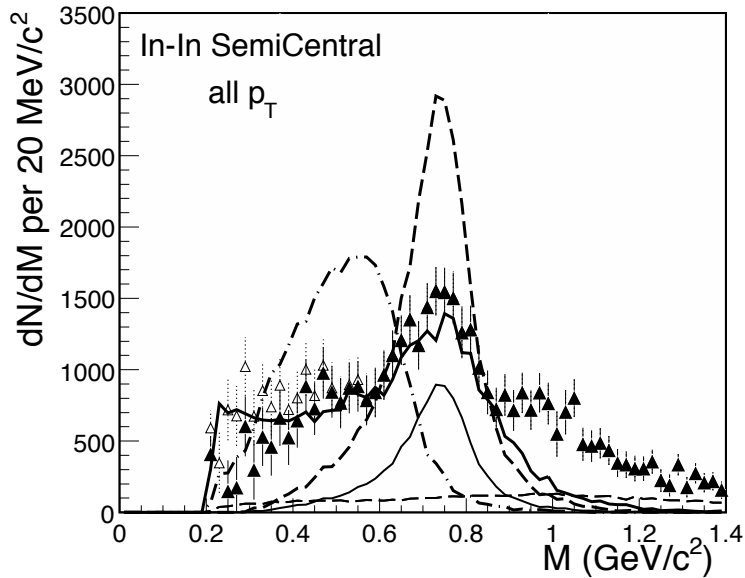


Figure 25: ρ spectral function measurement at by NA60 at $\sqrt{s} = 17$ GeV[31] compared to several theoretical models. Note the mass bin size of 25 MeV/c².

PHENIX measurement of the spectral function would have similarly-sized error bars to those of NA60 in the same binning.

5.6.3 Search for opacity onset between 22 and 62.4 GeV

Signatures of the onset of opacity include R_{AA} of π^0 to measure the medium's opacity to light quarks and R_{AA} of non-photonic single electrons to explore opacity to charm. PHENIX is able to trigger on both of these, which is necessary for accumulation of comparison data in p+p and, eventually, in d+Au collisions. Modifications of the di-hadron correlation functions provide additional complementary probes of medium opacity. Collecting sufficient statistics with these three observables is the basis to evaluate the required running time for this program.

Table 4 shows the estimated number of events required for each of these signatures, over a wide range of collision energies. The estimates are based upon past experience with such analyses in PHENIX, expected production rates, and minimum acceptable kinematic reach. R_{AA} measurements up to at least $p_T = 5$ GeV/c for both pions and electrons are required in order to study jet fragments, rather than particles emitted from the collectively flowing bulk of the medium. For the pions, the event requirement was obtained by requiring 30 counts in the 4-5 GeV/c p_T bin for 0-10% collisions. Two different assumptions were used for energy scaling, derived from actual yields observed in 62 and 22 GeV CuCu data. These result in the range given in Table 4. For non-photonic

electrons, the event requirements were obtained by scaling data sizes needed for previous analyses according to the expected energy dependence of the yield. Event estimates for di-hadron correlations were made assuming x_T scaling, and minimum statistical precision based upon the existing 30M event sample from the Run-4 62.4 GeV data.

$\sqrt{s_{NN}}$	$\pi^0 R_{AA}$	electron	di-hadron
100 GeV		75M	19M
60 GeV		260M	30M
39 GeV	$\approx 25\text{-}30\text{M}$	780M	
28 GeV	$\approx 45\text{-}60\text{M}$		65M
22 GeV	$\approx 75\text{-}125\text{M}$	$\approx 2\text{B}$	100M
12.3 GeV			150M
8.8 GeV			215M
7.6 GeV			245M
5 GeV			375M

Table 4: Required number of events for Au+Au collisions at different collision energies, for three different opacity observables.

Measurements of R_{AA} require p+p collision data at the same energy for the denominator. The required number of p+p events is driven by the $\pi^0 R_{AA}$ for energy below 62.4 GeV, and by the baseline measurement of non-photonic single electrons at and above 62.4 GeV. The required number of p+p events sampled by PHENIX triggers is 2B, 6.5B, 750M, 1.2B and 2.5B for $\sqrt{s} = 100, 60, 39, 28,$ and 22 GeV, respectively. We note that existing data on ion collisions at 22.4 GeV lack comparison p+p data from RHIC; the observed onset makes it compelling to make this measurement and remove uncertainties inherent in using data from the ISR as the denominator in R_{AA} . Though PHENIX has p+p data at 62.4 GeV, it is insufficient to provide the baseline measurement for non-photonic electrons. We note that the running times for the higher energy data sets are quite short, and believe that a half week period should suffice for changeover time and data collection.

Di-hadron correlations require d+Au running to establish k_T ; d+Au comparison data is also important to establish the magnitude of cold nuclear matter effects that flatten the hadron p_T spectra (i.e. to calibrate the Cronin effect, that acts in opposition to suppression by the medium). As we anticipate a delay before d+Au comparison runs can be done, we request Au+Au collisions at approximately 39 and 28 GeV, where existing data on p+A collisions at Fermilab provide information on the Cronin effect for hadrons. Collecting the corresponding d+Au data will take less than a week at 100 GeV, but would require as much as 56 weeks at 22 GeV, as yields decrease as \sqrt{s} and luminosity falls as s .

Using these requirements, we propose an energy scan to search for onset of the perfect liquid in Run-10 as shown in Table 5. Our highest priority is new energy points at $\sqrt{s_{NN}} =$

38.8 (or 39) and then 28 GeV. There is a strong discovery potential argument to make this scan in Run-10, and to begin with heretofore unexamined energies. We understand that such a scan is best performed by moving from highest to lowest energy, according to the C-A D guidance, and that we should count upon 2 days transition time to each energy.[32] While the 28 GeV running is compelling, it does require a substantial number of weeks to collect these data. Consequently, we have considered a contingency plan should the Run-10 energy scan be curtailed. Under such a constraint we would prefer postponing the 28 GeV run to collecting a data set too small to allow decisive measurement of the compelling signatures. We would propose instead 1 week of running at 100 GeV, along with the corresponding p+p baseline measurement (which requires only a few days), to probe the onset of charm suppression at RHIC.

	$\sqrt{s_{NN}}$	weeks	events	comment
cooldown		2		
p+p start/rampup	500	3		
p+p physics	500	5		record 25pb ⁻¹
	62.4	0.5	6.5B	comparison
	39	0.5	≈1B	
	28	0.5	1.2B	
	22.4	1.0	2.5B	
Au+Au startup	62.4	2		
Au+Au energy changes	39, 28	0.5		
Au+Au physics	62.4	2	300M	
	39	5	300M	no charm measurement
	28	7.5	100M	
warm-up		0.5		
TOTAL		30		

Table 5: Plan for Run-10 energy scan for perfect liquid onset.

5.6.4 Search for critical point at lower energies

In the search for the QCD critical point it would be ideal to collect substantial data sets at most of the collision energies listed in Table 3. 100 M events at each energy would allow measurement of di-electrons and di-hadron correlations. Given the baseline luminosity *and collision vertex length* projections, such data sets are only feasible above transition energy (and above SPS top energy). A potential approach could be to collect a substantial dataset for one collision energy that overlaps with the SPS. However, even at the highest SPS energy this would consume a prohibitively large fraction of one year's running time.

# events	Signatures that become available
1 M	$\langle N_{ch} \rangle$ (integral), $\langle p_T \rangle$ fluctuations, min bias PID spectra
5 M	PID vs. centrality, minimum bias v_2
50 M	v_2 vs. centrality, "basic" HBT, di-electrons
100 M	$\pi^0 R_{AA}$ (Full centrality dependence), di-hadrons

Table 6: Signatures accessible with different event sample size.

The impact of limited data set size can be seen from Table 6, which shows the critical point signatures within reach for different magnitude event samples at $\sqrt{s_{NN}} = 20$ GeV. Below transition, multiple datasets of only a few million events are realistically possible. With such datasets PHENIX can measure $\langle N_{ch} \rangle$ and $\langle p_T \rangle$ fluctuations and identified particle spectra with limited centrality selection. Though these would allow a search for non-statistical fluctuations in particle production and analysis with thermal models of hadron gas freezeout, it is unclear how competitive such data sets would be with those already produced by SPS experiments. Furthermore, operating RHIC experiments in a regime that does not provide for a wide variety of observables to characterize the system, and lacking robust comparison p+p and d+Au data, would represent a major deviation from the approach to discovery science that has proven so successful at RHIC.

At energies above transition, but below full energy, RHIC is poised to make a unique and substantial contribution to the low baryon chemical potential end of the critical point search. This requires similar conditions to quantification of the onset of light-quark and heavy-quark opacities. With less than 20 weeks of running, substantial datasets (300 M events) can be collected at several different energies (22.4, 28, 39, 62.4 and 100 GeV), allowing analyses of many possible signatures. We propose that the scan described in the section above is also the right first step toward locating the critical point at RHIC.

Since the critical point is theoretically expected to be at the lower end of viable RHIC energies, a substantial data set at 22.4 GeV would seem to optimize discovery potential. On the other hand, a small dataset has already been collected at this energy, so there is appeal to first run at intermediate energy. At energies above transition there is not much expected run-time difference for run 2012 compared to 2010 for PHENIX, as the expected increase in luminosity is offset almost exactly by the reduced z vertex acceptance. Thus, the luminosity does not dictate whether 22.4 GeV should be run in 2010 or later. However, detector upgrade considerations are important. For the first low-energy running period, in 2010, there is a reasonable likelihood that the the HBD and the RXNP detectors will be in place; unless it proves possible to accomplish the full Run-9 goals prior to summer 2009. For the second low-energy running period these detectors will be removed and the VTX will be in place.

Both of these central detector sets have triggering capability and supplement the BBC at lower energies. The vertex detector will offer improved centrality determination and

multiplicity fluctuation measurements, as its acceptance is far larger than that of the PHENIX central arms. This argues for deferring running of low luminosity collisions until the VTX is installed.

There is much more physics that could be obtained with higher luminosities and a low-frequency SRF upgrade. However, given the existing SPS datasets, it is not clear that funding for such upgrades is a top priority. On the other hand, it may be that a lot of the interesting physics could be obtained through measurements of smaller systems at full RHIC energy. Such an approach effectively varies the energy density, while keeping the baryochemical potential approximately fixed. As the CERN experiments find any evidence for anomalous fluctuations in peripheral, but not for central collisions, system size is clearly important. Varying system size may, in fact, be as compelling as varying \sqrt{s} in central Au+Au collisions. Furthermore, the study of smaller systems at full energy is much better suited to RHIC's luminosity and collision vertex capabilities. Such an approach would also better utilize PHENIX's strengths in rate capability.

6 Beam Use Proposal for Run-9 and Beyond

6.1 Planning Assumptions and Methodology

The Associate Laboratory Directory for Nuclear and High Energy Physics has directed the experiments to produce a 5 year running plan assuming 25 weeks of cryo operations in Run-9 and 30 cryo weeks per year in the out years.

Detailed guidance provided by the Collider-Accelerator Department (C-A D) describes the projected year-by-year luminosities for various species, along with the expected time-development of luminosity in a given running period[32]. We have used the species-dependent luminosity guidance, the stated cool-down time, and the stated start-up and ramp-up time for each species to convert the required delivered integrated luminosities into a plan for the approximate number of weeks at each species. The by-now extensive experience with operating RHIC in a variety of modes and in understanding luminosity limitations provides some confidence in the projected minimum luminosities, which are based on either actual experience or achieving the same charge per bunch as for Au beams. Maximum projected luminosities are based on current understanding of the accelerator limits. As in past beam use proposals, we use the geometric mean of the minimum and maximum projected luminosities. We applaud the C-A D efforts to develop stochastic cooling, and support running full energy Au+Au to support this development, as well as to provide data for our ongoing physics program.

Our ambitious goals for spin observables have led PHENIX to request annual opportunities to further develop luminosity and polarization for p+p collisions. Run-9 is impacted

by the lack of p+p running in Run-7 and the curtailed running in Run-8, where insufficient time was available for luminosity and polarization development. We are anxious to resume progress toward the projections used in the Spin Research Plan[11] submitted to DOE in February, 2005.

Based on the CA-D guidance for Run-9 luminosity [32], we assume the following figures on luminosity and polarization for Run-9:

- The delivered (integrated) luminosity in $\sqrt{s}=200$ GeV run will be between 40 pb^{-1} and 100 pb^{-1} for 10 weeks. We use 70 pb^{-1} in this Proposal. With a factor of $\sim 1/3$ (which includes DAQ lifetime, Z-vertex cut etc.) we arrive at 21 pb^{-1} recorded (integrated) luminosity. This may increase by a factor 1.2–1.3 due to improved PHENIX vertex cut “efficiency” after the new 9 MHz rf system is installed, leading to a reduction of bunch length by a factor $\sqrt{2}$ (this PHENIX specific vertex cut efficiency improvement is of course not included in [32]). According to [32] store average polarization of 65% will be reliably demonstrated, but expected average store polarization after 2.5 weeks of set-up and ramp-up will be 40%. So finally we used $L=25 \text{ pb}^{-1}$ and $P=60\%$ for our projections below.
- Assuming that a $\sqrt{s}=500$ GeV run will directly follow the $\sqrt{s}=200$ GeV run and that a number of machine developments will be successfully finished before the $\sqrt{s}=500$ GeV run starts, we may expect to get roughly 7–9 pb^{-1} per week at $\sqrt{s}=500$ GeV. This includes the factor 2.5 higher luminosity compared to $\sqrt{s}=200$ GeV due to emittance shrinkage at the higher beam energy). Consequently, leaving 2 (of 5) weeks for machine set-up, we may expect $\sim 25 \text{ pb}^{-1}$ for 3 weeks of physics running at $\sqrt{s}=500$ GeV. The expected polarization might be lower than at $\sqrt{s}=200$ GeV due to a number of additional depolarizing resonances in RHIC when accelerating protons between 100 and 250 GeV.

In order to convert delivered luminosities from the C-A D projection document into recorded luminosities, we use recent experience to estimate the effects of the PHENIX vertex requirement of $|z| < 30$ cm, and the PHENIX data acquisition system up-time. The PHENIX up-time has improved substantially in the past year due to improved DAQ rate and Run Control, as well as faster run start-up by the shift crews. This document uses the new combined conversion factor of 33% to calculate recorded luminosities from the delivered values.

For energies between the injection energy (20 GeV) and full energy, RHIC luminosity scales as $L \approx E^2$. For even lower energies the expected luminosity is unknown, although it is expected to fall even faster. Furthermore, for energies below the injection energy the storage RF (which reduces the collision vertex z-spread) cannot be used. Therefore the RMS of the z vertex for those low energies will increase to $\sigma \approx 150\text{cm}$, resulting in further significant luminosity reduction. To get the projected *delivered* luminosity at lower ener-

gies we used the average of the minimum and maximum luminosity[32] and multiplied by $(E/200)^2$ the most optimistic energy scaling. To obtain the recorded Au+Au luminosity, we corrected for PHENIX up-time (70%), live-time (90%), trigger vertex efficiency (variable, see below), trigger efficiency inside the vertex (96% - simulated efficiency for the RXNP trigger down to 10 GeV), assumed efficiency for the VTX minimum bias trigger), offline QA efficiency (85%) and offline vertex cuts (90%). There is a significant reduction in the collected luminosity due to the relatively large collision z vertex rms compared to the PHENIX acceptance. With the full voltage from the 200 MHz SRF, and longitudinal stochastic cooling, the expected z vertex rms above transition energy (20 GeV) is 20 cm. Below transition the SRF cannot be used, resulting in bunches with full longitudinal size and z vertex rms = 150 cm. Given these values and the PHENIX vertex acceptance (± 30 cm pre-VTX (2010) and ± 10 cm post-VTX (2012)) we use vertex acceptance of 0.68 (0.99) with (without) VTX cuts with SRF, and vertex acceptance of 0.11 (0.31) with (without) VTX cuts with no SRF.

6.2 Beam Use Proposal Summary

This proposal aims to maintain the program of discovery physics that has attracted worldwide attention to the RHIC heavy ion program, *while maintaining* progress in the spin physics program and development of polarized proton performance. This is best accomplished by

- Continued enrichment of existing data sets that are statistically sparse in essential physics channels (which requires accumulation of data over multi-year periods)
- Optimizing the RHIC run plan to take advantage of key detector upgrades as they become available.
- Targeting physics goals to utilize RHIC luminosity and ion source improvements in both the heavy ion and spin programs. This consideration is also critical running below injection energy.
- Continued development of luminosity and polarization for decisive measurements with polarized protons.
- *Completing* surveys by securing requisite baseline data in a timely fashion, so that comparison data sets are obtained with essentially the same detector configuration.

Table 7 summarizes the current PHENIX Beam Use Proposal. The major features are:

- Our highest priority for Run-9 is polarized proton running. The first goal is to record sufficient integrated luminosity with longitudinal polarization to provide a sensitive measurement of the gluon polarization of the proton via 200 GeV p+p collisions.
- Au+Au running at $\sqrt{s_{NN}} = 200$ GeV in Run-9 to complete the required large data set (order of magnitude increase over Run-4) for rare probes that was begun in Run-7. This run also will allow precision measurement of low mass dileptons with background rejection by the HBD.
- Begin 500 GeV polarized proton operations, and allow first observations of W bosons in PHENIX to meet the RIKEN milestone in March 2011. Collect a large 500 GeV data set over several years once the muon trigger upgrades are fully operational.
- Au+Au collisions at a number of energies below 200 GeV, collected over two or more years. The first goal is to find the onset of medium opacity and maximal collective motion, and measure the other medium properties at that point. The second goal is to search for evidence of the QCD Critical Point, aided by enhanced acceptance once the VTX detector is installed.
- High statistics full energy Au+Au running, plus p+p comparison data utilizing the silicon detector upgrades.
- U+U collisions at full RHIC energy to explore the maximum energy density.

Table 7: The PHENIX Beam Use Proposal for Runs 9-13. We note that the "OR" in Run-10, which results from uncertainties in Run-9, would imply revision of the remainder of Run-10.

RUN	SPECIES	$\sqrt{s_{NN}}$ (GeV)	PHYSICS WEEKS	$\int \mathcal{L} dt$ (recorded)	p+p Equivalent
9	p+p	200	10	25 pb ⁻¹	25 pb ⁻¹
	<i>OR</i> p+p	500	5	25 pb ⁻¹	25 pb ⁻¹
	Au+Au	200	10	1.4 nb ⁻¹	56 pb ⁻¹
10	p+p	500	5	25 pb ⁻¹	25 pb ⁻¹
	<i>OR</i> p+p	200			
	p+p Au+Au	62.4, 39, 28, 22.4 62.4, 39, 28	2.5 15		
11	Au+Au	200	M		
	p+p	500	25-M		
12	U+U	200	N		
	p+p	200	25-N		
13	p+p	500	Q		
	Au+Au	various	25-Q		

The Run-4 and Run-7 data sets for full energy Au+Au collisions resulted in critical new observations. However, over substantial regions of interest the statistical errors exceed the systematic errors. Correspondingly, the ability to address fundamental questions (e.g., does the flow extend to bottom quarks?) is limited by the statistical reach of the existing data sets; increased statistics will also help decrease a number of the systematic uncertainties. Crucial rare event physics that we are only beginning to address include the flow of J/Ψ 's (perhaps a critical test of regeneration mechanisms), photon+jet measurements, direct photon flow (again, which may be a critical test for QGP-induced bremsstrahlung and/or conversion mechanisms) and 3-particle jet correlations. The Run-7 data set alone is insufficient to resolve these questions. Consequently, an order of magnitude increase in integrated luminosity by adding together Run-7 and Run-9 data sets is proposed.

While there is great value to be derived from a multi-year planning process, we are also aware of the intrinsic limitations when such plans are confronted with ongoing discovery physics, machine development schedules, and uncertain funding scenarios. Accordingly, we have indicated the Collaboration's priorities among species proposed for the first two years of this proposal. Furthermore, we have identified two distinct, though related, goals for ion collisions at lower energy. The first is to discover the onset of medium opacity to light and heavy partons. As this is known to occur between 62.4 and 22 GeV, at least for light quarks and gluons, this search can be undertaken prior to RHIC luminosity increases. Exploration of the landscape of baryochemical potential for evidence of the QCD critical point will likely require running at energies below injection energy. As the luminosity is low and collision vertex very long at these energies, such studies will benefit greatly from luminosity increases. Consequently, we propose to pursue this goal second.

The requested sequence of runs is motivated by and coordinated with the program of upgrades. In particular, Run-9 will provide the low-mass dilepton physics made possible by the HBD. Following this, commissioning of the VTX detector will begin, leading to separated charm and bottom physics in 2011.

Addition of the FVTX and then NCC will allow PHENIX to perform the long awaited quarkonium spectroscopy measurements to probe color screening in the medium. High luminosity RHIC operations in 2012 will add upson statistics to provide a crucial test with a very small bound state. It should be noted that the need for equivalent p+p integrated luminosity to provide adequate baseline data for the heavy ion program will also provide data toward our goals for spin measurements at 200 GeV and also at somewhat lower energy.

6.3 Run-9

The highest priority for the PHENIX Collaboration in Run-9 is to collect data with polarized protons, preferably at 200 GeV. Our goal is to record 25 inverse picobarns of data;

we estimate that this will require 10 weeks of physics running. Should a Continuing Resolution prohibit 10 weeks of physics plus the necessary 5 weeks cooldown/setup/rampup before the end of June, PHENIX requests instead a first run of 500 GeV polarized proton collisions. In this event 3-4 weeks of physics running should be sufficient for first measurements of production cross-sections, background rates, and an initial W asymmetry measurement. The p+p collision energy that is not run in Run-9 would then be a priority for Run-10.

Our second priority for Run-9 is to record approximately 1.4 inverse nanobarns of Au+Au collisions to complete the large Au+Au data set and provide low mass dilepton spectra. As the Hadron Blind Detector cannot coexist in PHENIX with the silicon vertex detector currently under construction, it is imperative to collect the required data before the vertex detector is complete.

6.3.1 Polarized proton collisions

PHENIX requests 15 weeks of Physics Operations with polarized protons in Run-9: 10 weeks for longitudinal collisions at PHENIX at $\sqrt{s}=200$ GeV and 5 weeks for longitudinal collisions at PHENIX at $\sqrt{s}=500$ GeV. We assume that 3 additional weeks are required for set-up and ramp-up of RHIC for the first polarized proton energy, and 2 weeks for the second. The PHENIX goal is to record 25 pb⁻¹ of 200 GeV collisions with polarization of at least 60%. The 500 GeV integrated luminosity goal is 25 pb⁻¹ with 60% polarization.

We note that progress toward the RHIC design luminosity and polarization requires substantial running time. The experience with the short polarized proton run in Run-8 underscores the need to run the machine for a prolonged period in order to develop stable high performance run conditions. PHENIX also requests that the Collider-Accelerator Department prepare the 9 MHz cavity to improve delivered luminosity, devote the required effort to optimize the polarization, and develop the spin flipper for Run-9 to enable better control of systematic uncertainties.

PHENIX considers the the minimum “reasonable” length of a longitudinal $\sqrt{s}=200$ GeV run to be 8 weeks. We note that the loss in the figure of merit, LP^4 , could be considerably larger than 20%, compared to 10 weeks running, as the final few weeks of any run usually provide with highest luminosity and polarization. Should the available Run-9 Physics weeks be fewer than 8, we request instead that Run-9 be devoted to $\sqrt{s}=500$ GeV operations.

6.3.2 8-10 weeks Au+Au collisions at $\sqrt{s_{NN}} = 200$ GeV

PHENIX requests 8-10 weeks of full energy Au+Au collisions to record $\int L dt = 1.4 \text{ nb}^{-1}$. Though we expect this to require the full 10 weeks, the collaboration would likely be willing to accept a somewhat lower integrated luminosity of 1.2 nb^{-1} in order to ensure that these data are collected during Run-9. We believe that 8 weeks of Physics is a minimum, however. This run will complete our large Au+Au data set for the study of rare probes, and provide a data set for dielectron measurements with the HBD.

6.4 Run-10

For Run-10, the highest priority of the PHENIX Collaboration is to complete the second p+p goal. If 200 GeV p+p is completed in Run-9, we request 500 GeV p+p collisions early in Run-10 in order to meet the RIKEN March 2011 milestone for first observation of W's. Our second priority in Run-10 is to begin the search for onset of the perfect liquid in Au+Au collisions at energies between 62.4 and 22 GeV per nucleon pair.

PHENIX proposes 5 weeks of Physics running with polarized protons at $\sqrt{s} = 500$ GeV, in order to begin the W program. This first run will be used to measure the cross sections for various processes at this new energy, measure the background in the muon arms under the W and test the impact of a prototype hadron absorber, and as an engineering run for new muon trigger hardware. We anticipate publishable measurements of unpolarized cross sections and a first look at the W longitudinal spin asymmetry.

The second priority is an energy scan to search for onset of the perfect liquid in Run-10 as shown in Table 5. The highest priority is the new energy point at $\sqrt{s_{NN}} = 38.8$ (or 39) GeV. However, we indicate in the table a plan arranged for maximum operational efficiency of RHIC.[32] When the actual number of cryo weeks for Run-10 is known, the running split will likely need to be revisited. Furthermore, we anticipate the pixel layers of the VTX will be available by Run-10. Consequently, Run-10 could provide an engineering run for the VTX; with a short 200 GeV run segment, we can test the ability of the detector for b/c separation. Due to the b production cross section, this test would be difficult at lower energy.

6.5 Run-11

By Run-11, the PHENIX central barrel silicon vertex detector will be completed and installed. Consequently, we request full energy Au+Au collisions to make first measurements of charm and bottom separately.

	$\sqrt{s_{NN}}$	weeks	events	comment
cooldown		2		
p+p start/rampup	500	3		
p+p physics	500	5		record 25pb ⁻¹
	62.4	0.5	6.5B	comparison
	39	0.5	≈1B	
	28	0.5	1.2B	
	22.4	1.0	2.5B	
Au+Au startup	62.4	2		
Au+Au energy changes	39, 28	0.5		
Au+Au physics	62.4	2	300M	
	39	5	300M	no charm measurement
	28	7.5	≈ 250M	
warm-up		0.5		
TOTAL		30		

Table 8: Plan for Run-10. (Table 5 is repeated here for convenience.)

PHENIX also expects all muon trigger hardware to be fully installed for this run, and so we request the first long production run of polarized protons at 500 GeV.

6.6 Run-12

Though it is difficult to make long-baseline projections, we nonetheless note that completion of the EBIS project in this period will provide the unprecedented opportunity to study U+U collisions. The static quadrupole deformation of the uranium nucleus will lead to collisions (in some orientations) with significantly greater initial densities than those found in Au+Au collisions, presenting new challenges to both theory and experiment to extract and understand the influence of the initial geometry on the subsequent dynamics. Consequently, we propose (25-N) weeks “heavy ion” running at $\sqrt{s_{NN}} = 200$ GeV.

Our next priority for Run-12 is to return to 200 GeV p+p collisions. These data will provide the baseline measurement for heavy quark physics with the VTX and FVTX detectors. It will also add precision to our earlier measurements of ΔG at 200 GeV, allowing PHENIX to use direct photon production to probe ΔG . The exact split of the running time between the two species will be evaluated when the expected machine performance is better known.

6.7 Run-13

As in 200 GeV polarized proton program, we project steady accumulation of integrated luminosity at 500 GeV over a multi-year period. X weeks p+p longitudinal polarization at 500 GeV will contribute to this program. The Nose Cone Calorimeter and the Forward Vertex detectors will also be available at this time, once again extending the PHENIX physics reach for both the polarized proton and heavy ion programs.

In addition to the continuation of the 500 GeV polarized proton program, PHENIX requests additional low energy Au+Au running at several energies lower than those of Run-10. This running is with the goal of finding experimental evidence for the QCD critical point. The VTX detector will greatly enhance our acceptance for charged particles, allowing a much higher precision search for fluctuation signatures of the critical point than with the central arms alone.

References

- [1] Initial PHENIX Run-1 request, 24-May-99,
<http://www.phenix.bnl.gov/phenix/WWW/publish/zajc/sp/presentations/RBUP99/rbup99.htm>
- [2] PHENIX Run-1 presentation to PAC, 23-Mar-00,
<http://www.phenix.bnl.gov/phenix/WWW/publish/zajc/sp/presentations/RBUP00/rbup00.htm>
- [3] PHENIX Run-2 presentation to PAC,
<http://www.phenix.bnl.gov/phenix/WWW/publish/zajc/sp/presentations/RBUPNov00/RBUPNov00.htm>
- [4] PHENIX Run-2 proposal for extended running:
<http://www.phenix.bnl.gov/phenix/WWW/publish/zajc/sp/presentations/RBUPSep01/RBUPSep01.html>
- [5] PHENIX Runs 3-5 proposal to PAC, Aug-02,
<http://www.phenix.bnl.gov/phenix/WWW/publish/zajc/sp/presentations/RBUPAug02/RBUPforAug02PAC.pdf>
- [6] PHENIX Beam Use Proposal for RHIC Runs 4-8, Sep-03,
<http://www.phenix.bnl.gov/phenix/WWW/publish/zajc/sp/presentations/RBUP03/ProposalText/RBUPforRuns4-8.pdf>
- [7] PHENIX Beam Use Proposal for RHIC Runs 5-9, Jul-04,
<http://www.phenix.bnl.gov/phenix/WWW/publish/zajc/sp/presentations/RBUP04/ProposalText/RBUPforRuns5-9.pdf>

- [8] PHENIX Beam Use Proposal for RHIC Run-6 and Beyond, Oct-05,
<http://www.phenix.bnl.gov/phenix/WWW/publish/zajc/sp/presentations/RBUP05/ProposalText/RBUPforRun7andBeyond.pdf>
- [9] PHENIX Beam Use Proposal for RHIC Run-7 and Beyond, Sep-06,
<http://www.phenix.bnl.gov/phenix/WWW/publish/zajc/sp/presentations/RBUP06/ProposalText/RBUPforRun7andBeyond.pdf>
- [10] PHENIX Beam Use Proposal Update for RHIC Run-7 and Beyond, Mar-07,
http://www.phenix.bnl.gov/phenix/WWW/publish/jacak/sp/RBUP07/RBUP07_update.pdf
- [11] Research Plan for Spin Physics at RHIC, submitted to U.S. Department of Energy February, 2005; available from <http://spin.riken.bnl.gov/rsc/report/masterspin.pdf>
- [12] A. Adare, et al. (PHENIX Collaboration) arXiv:0801.4555, submitted to Phys. Rev. Lett. (2008).
- [13] I. Vitev, Phys. Lett. **B639**, 38 (2006).
- [14] A. Adare, et al.(PHENIX Collaboration) arXiv:0801.0220, submitted to Phys. Rev. Lett. (2007).
- [15] A. Adare, et al.(PHENIX Collaboration), arXiv:0801.4020 submitted to Phys. Rev. Lett. (2008).
- [16] A. Adare, et al.(PHENIX Collaboration) arXiv:0801.1665, submitted to Phys. Rev. C (2008).
- [17] A. Adare, et al.(PHENIX Collaboration) arXiv:0801.4545, submitted to Phys. Rev. C (2008).
- [18] S. Afanasiev, et al.(PHENIX Collaboration) arXiv:0712.4372, submitted to Phys. Rev. Lett. (2007).
- [19] A. Adare, et al.(PHENIX Collaboration) (arXiv:0802.0050). submitted to Phys. Lett. B. (2008).
- [20] K. Boyle, presentation at the AGS&RHIC User's meeting, BNL, June 2007.
- [21] B. Jäger *et al.*, Phys. Rev. **D67**, 054005 (2003); M. Glück *et al.*, Phys. Rev. **D63**, 094005 (2001).
- [22] Daniel de Florian, Rodolfo Sassot, Marco Stratmann and Werner Vogelsang, arXiv:0804.0422 (2008).
- [23] Daniel de Florian, Beller Lecture, APS Meeting St. Louis, April 13, (2008).
- [24] K. Adcox, et al. (PHENIX Collaboration), Nucl.Phys. **A757**, 184 (2005).

- [25] Jorge Casalderrey-Solana and Derek Teaney, Phys. Rev. **D74**, 085012 (2006).
- [26] W.A. Horowitz and M. Gyulassy, arXiv:0706.2336 (2007).
- [27] A. Adare, et al.(PHENIX Collaboration) Phys. Rev. Lett. **98**, 172301 (2007).
- [28] S. S. Adler, et al.(PHENIX Collaboration) Phys. Rev. Lett. **94**, 232302 (2005).
- [29] K. Rajagopal, "Can We Discover the QCD Critical Point at RHIC?," RHIC 2006 Critical Point Workshop, <https://www.bnl.gov/riken/QCDRhic/talks.asp>.
- [30] S. Afanasiev, et al.(PHENIX Collaboration) arXiv:0706.3034, submitted to Phys. Rev. Lett. (2007).
- [31] R. Arnaldi, et al. (NA60 Collaboration), Phys. Rev. Lett. **96**, 162302 (2006).
- [32] RHIC Collider Projections (FY2009-FY2013), W. Fischer *et al.*, last updated February 23, 2008 available from <http://www.agsrhichome.bnl.gov/RHIC/Runs/RhicProjections.pdf>.